Comprehensive REVIEWS in Food Science and Food Safety

Emerging Spectroscopic and Spectral Imaging Techniques for the Rapid Detection of Microorganisms: An Overview

Kaiqiang Wang, Hongbin Pu, and Da-Wen Sun

Abstract: Microorganism contamination and foodborne disease outbreaks are of public concern worldwide. As such, the food industry requires rapid and nondestructive methods to detect microorganisms and to control food quality. However, conventional methods such as culture and colony counting, polymerase chain reaction, and immunoassay approaches are laborious, time-consuming and require trained personnel. Therefore, the emergence of rapid analytical methods is essential. This review introduces 6 spectroscopic and spectral imaging techniques that apply infrared spectroscopy, surface-enhanced Raman spectroscopy, terahertz time-domain spectroscopy, laser-induced breakdown spectroscopy, hyperspectral imaging, and multispectral imaging for microorganism detection. Recent advances of these technologies from 2011 to 2017 are outlined. Challenges in the application of these technologies for microorganism detection in food matrices are addressed. These emerging spectroscopic and spectral imaging techniques have the potential to provide rapid and nondestructive detection of microorganisms. They should also provide complementary information to enhance the performance of conventional methods to prevent disease outbreaks and food safety problems.

Keywords: hyperspectral imaging, infrared spectroscopy, laser-induced breakdown spectroscopy, microorganism, multispectral imaging, surface-enhanced Raman spectroscopy, terahertz time-domain spectroscopy

Introduction

Microorganisms, including bacteria, fungi, and viruses, in food products are closely associated with the quality and safety of food, and they have become a public concern throughout the world (Fan and others 2011; Cheng and Sun 2015a). With the globalization of food production and commerce, the manufacture and distribution of food has become a universal and interconnected system. However, nearly a quarter of the global food supply is damaged through microbial activity alone, and microbiological contamination has become the most common source of foodborne diseases (Papadopoulou and others 2011). Microorganisms in food products during processing and storage can cause mortality, morbidity, food spoilage, and economic loss, and thereby imperil food quality and human safety (Calvo and others 2010; Siripatrawan and others 2011). As pathogenic microorganisms have the ability to live inside host cells, foods infected by pathogenic microorganisms may result in severe health consequences for consumers. Therefore, common preservation techniques such as drying (Sun 1999; Delgado and Sun 2002; Pu and Sun 2016; Ma and others 2017; Pu and Sun 2017; Qu and others 2017; Yang and others 2017), cooling (Sun 1997; McDonald and others 2001; Wang and Sun 2001; Wang and Sun 2004; Sun and Zheng 2006) and freezing (Kiani and others 2011; Kiani and others 2012; Ma and others 2015; Pu and others 2015; Xie and others 2015; Cheng and others 2016; Xie and others 2016; Cheng and others 2017) are often used to maintain food quality and safety on the other hand, the establishment of effective detection methods and the suppression of risks from microbiological contamination are also of very importance to the food industry and to public health. Conventional microorganism detection methods, such as culturing and colony-counting methods (Chen and others 2003), polymerase chain reaction methods (Olaoye and others 2011), and immunoassay approaches (Magliulo and others 2007), are capable of detecting initially low numbers of cells and have limited requirements of specialized apparatus (Feng and Sun 2013b). Nevertheless, these methods are normally laborious and destructive, and they also require well-trained operators and much time to obtain results. Furthermore, they cannot be employed for on-line monitoring of large numbers of samples. They are awkward for both the food industry and regulatory authorities, as foods with short shelf-life may suffer from spoilage before authentic results are obtained.

CRF3-2017-0165 Submitted 8/9/2017, Accepted 11/2/2017. *Authors are with School of Food Science and Engineering, South China Univ. of Technology, Guangzhou 510641, China. Authors are also with Acad. of Contemporary Food Engineering, South China Univ. of Technology, Guangzhou Higher Education Mega Center, Guangzhou 510006, China. Authors are also with Engineering and Technological Research Centre of Guangdong Province on Intelligent Sensing and Process Control of Cold Chain Foods, Guangzhou Higher Education Mega Center, Guangzhou 510006, China. Author Sun is also with Food Refrigeration and Computerized Food Technology (FRCFT), Agriculture and Food Science Centre, Univ. College Dublin, National Univ. of Ireland, Belfield, Dublin 4, Ireland. Direct inquiries to author Sun (E-mail: dawen.sun@ucd.ie).*

doi: 10.1111/1541-4337.12323

In order to overcome these drawbacks, the exploration of rapid analytical techniques has become an important research topic. The rapid development in nanomaterial, electronic, optical, and electrochemical sciences has led to a variety of novel analytical methods: flow cytometry (Fröhling and others 2012), mass spectrometry (Freiwald and Sauer 2009), electronic nose and electronic tongue (Kodogiannis 2017), biosensors (Park and others 2013), as well as spectroscopic and spectral imaging techniques (Lu and others 2011; Cheng and Sun 2015b; Mungroo and others 2016), all appropriate for the rapid detection of microorganisms. Spectroscopic and spectral imaging techniques have become popular and attractive due to minimal sample preparation and rapid data acquisition. Most of them can achieve nonabrasive, label-free, in situ, and on-line detection. However, no review is available that focuses on spectroscopic and spectral imaging techniques for microorganism detection. Therefore, the current review aims to introduce the principles of 6 emerging spectroscopic and spectral imaging techniques, including infrared spectroscopy (IRS), surface-enhanced Raman spectroscopy (SERS), terahertz time-domain spectroscopy (THz-TDS), laser-induced breakdown spectroscopy (LIBS), hyperspectral imaging (HSI), and multispectral imaging (MSI) for microorganism detection. As these techniques develop very rapidly, this review only covers their recent applications from 2011 to 2017. The review will provide a better understanding of the rapid detection of microorganisms in food matrices and encourage early adoption of these techniques in the food industry.

Spectroscopic Techniques

Infrared spectroscopy (IRS)

The infrared (IR) region covers frequencies in the electromagnetic spectrum ranging from 12500 to 33 cm^{-1}, which can be subdivided into near infrared (12500 to 4000 cm^{-1}), middle infrared (4000 to 400 cm^{-1}), and far infrared (400 to 33 cm^{-1}) (Zhang 2012). IRS is based on the radiation arising from the thermal emission of an appropriate hot source. If a particular motion is accompanied by a dipole moment change, then the corresponding chemical bonds or groups will absorb energies at frequencies corresponding to the molecular mode of vibration when they are illuminated with IR radiation. They will show a specific frequency in the IR spectrum (Alvarez-Ordonez and others 2011). Near-IR and mid-IR regions are often used for chemical analysis and have been employed for microorganism detection. Most chemical bonds, such as O–H, N–H, C═O, and C–H, absorb the characteristic frequencies of IR radiation in the mid-IR region. The incidence-spectral bands, as well as the intensity and the specificity of the signal, are higher in this region. Owing to fundamental transitions, a typical mid-IR spectrum offers absorbance peaks which roughly fall into 4 spectral windows defined as the X–H stretching region (4000 to 2500 cm^{-1}), the triple-bond region (2500 to 2000 cm^{-1}), the double-bond region (2000 to 1500 cm^{-1}), and the fingerprint region (1500 to 600 cm^{-1}) (Türker-Kaya and Huck 2017). Notably, the fingerprint region represents bands composed of unique broad and complex contours and is specific to the molecular structure of samples (Lin and others 2004; Wang and others 2017b). Unlike the mid-IR spectra, the absorption bands in the near-IR region originate from the overtones (secondary vibrations) of O-H, N-H, C-H, and S-H stretching vibrations or from stretching-bending combinations involving these groups. These are mostly affected by the formation of hydrogen bonds and can build characteristic spectra that behave as the fingerprint of the sample for chemical structure monitoring (Ozaki and others 2006). Although the molar absorptivity of the sample in near-IR is normally quite small, the IR radiation penetration depth increases as compared to that in the mid-IR region.

Microorganisms have unique chemical components (such as nucleic acids, proteins, carbohydrates, and fatty acids) in their cell membrane and cell wall, which can provide distinct IR absorption spectra. Nonetheless, most microorganisms appear to have similar IR spectra because of minor differences in their chemical compositions. As such, IRS technology combined with spectral pre-processing and different chemometrics is commonly applied for the quantification and the differentiation of microorganisms, and also for taxonomic level classification of food matrices (Davis and Mauer 2011; Tito and others 2012; Shapaval and others 2013a). Some commonly used spectral pre-processing methods include baseline correction, smoothing, normalization, and the first and second derivative transformations (Davis and Mauer 2010). After spectral pre-processing, chemometrics including partial least square regression (PLSR), stepwise multiple linear regression (SMLR), support vector machine (SVM), and artificial neural network (ANN) are employed for quantitative analysis. Principal component analysis (PCA), partial least squares (PLS), discriminant analysis (DA), random forest (RF), and least squares support vector machine (LS-SVM) are used for the discrimination and the classification of microorganisms. In order to evaluate the performance of prediction models, the correlation coefficients (R) and root mean square errors (RMSE) of a calibration set, a prediction set and cross-validation (R_c, R_p, R_{cv}; RMSEC, RMSEP, RMSECV) are calculated. A model with excellent prediction performance should have a high R, a low RMSE, and a small difference between RMSEC and RMSECV or RMSEP (Cheng and others 2017).

IRS has become a relatively mature technology for detecting groups of microorganisms due to its simplicity, rapidity, and applicability. To date, the spectral reference databases for various microorganisms have been established and validated, and some commercially manufactured IRS equipment for microbiology is available (Davis and Mauer 2010). In the past decade, IRS has been widely used for the discrimination and the classification of various microorganisms at the levels of species, subspecies, strains, serotype, and haplotype based on the IR absorbance patterns of cell components. For example, Davis and Mauer (2011) demonstrated the potential of IR combined with hierarchical cluster analysis (HCA) and canonical variate analysis (CVA) for discriminating *Listeria monocytogenes* at haplotype, serotype, and strain levels simultaneously, which gave a discrimination accuracy of 91.7%, 96.6%, and 100%, respectively. All of the classifications were completed within 18 h. In addition, a variety of research studies have shown evidence that IRS could be employed in the quality control of food products, such as the detection of pathogens (Alexandrakis and others 2011), the evaluation of food spoilage (Tito and others 2012), as well as the study of structural changes in microorganisms under stress conditions (Alvarez-Ordonez and others 2011).

However, most of the studies were carried out using expensive and bulky desktop instruments, which have relatively poor flexibility and adaptability for microbial determination in practical applications. Duan and others (2014) used a portable near-IR spectrometer for the rapid and nondestructive detection of total bacteria in flounder fillet. They combined genetic algorithm (GA) and back-propagation artificial neural network (BP-ANN) algorithms with IR spectra in the range of 600 to 1100 nm to develop the prediction model. These exhibited a better prediction efficiency (R = 0.985, RMSE = 0.095) than the usually exploited PLS model (R = 0.948, RMSE = 0.17). In order to

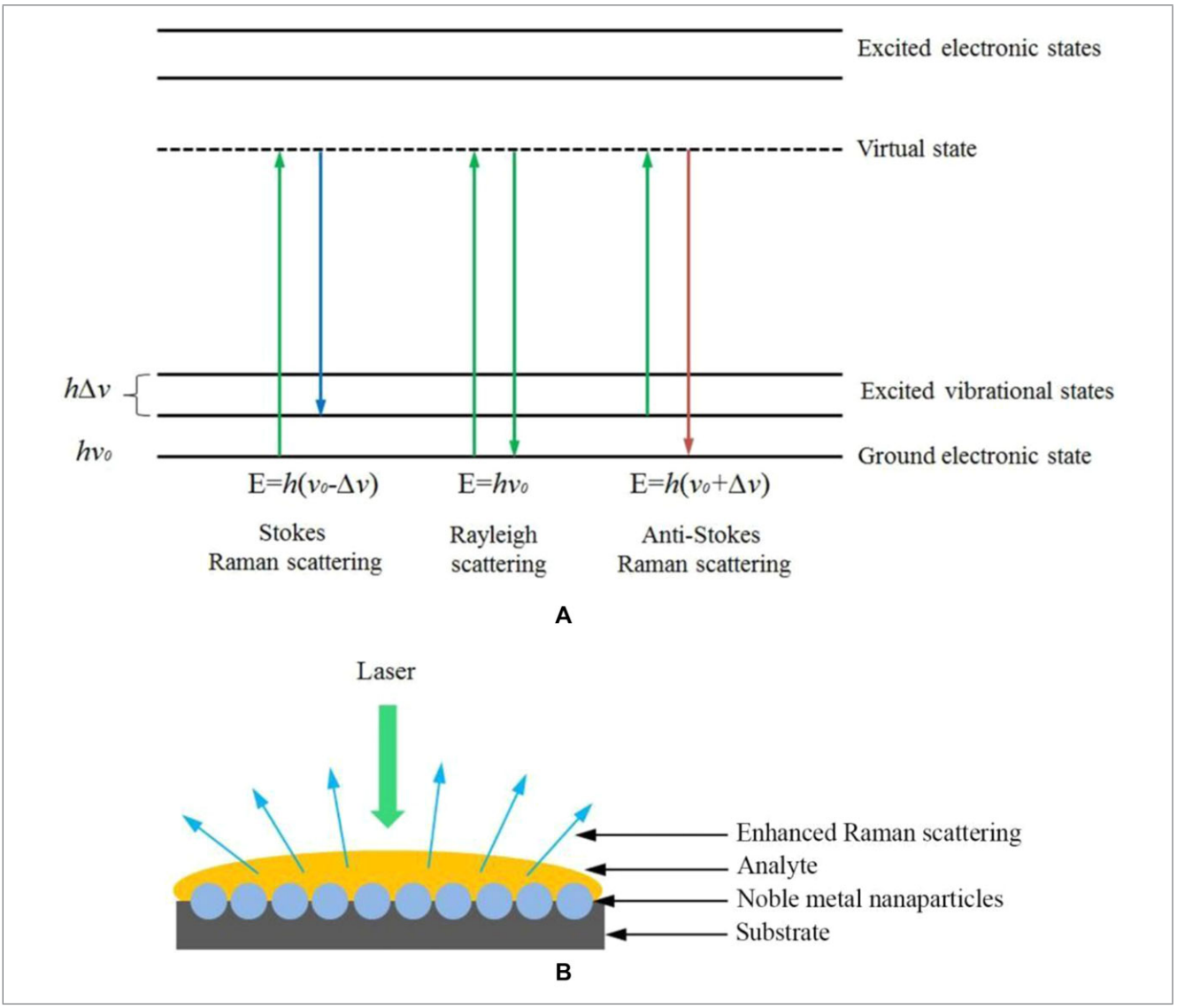

Figure 1–The mechanisms of (A) Raman scattering effect and (B) surface-enhanced Raman scattering effect.

make IRS suitable for industrial utilization, Shapaval and others (2013a) developed a high-throughput micro-cultivation protocol for the high-throughput Fourier transform infrared (FTIR) spectroscopic characterization and identification of molds depending on spectral libraries. Based on ANN analysis, the fungal samples were correctly identified with 94% accuracy at genus and species levels. Afterwards, authors established a novel library-independent approach based on high-throughput cultivation by FTIR spectroscopy for microbial source (20 spoilage mold strains) and 80% to 100% of the molds were correctly identified at the genus or species level (Shapaval and others 2016). The main advantage of the library-independent approach is that the contamination source can be identified, even if the microorganism is not represented by strains of the same species or genus in the spectral library. However, mycelium cultivation might be a limitation of that work (Shapaval and others 2016).

In most cases, the phenotypic expression of closely related microbial strains is difficult to differentiate by IRS due to their biochemical similarities and same responses to a standard growth medium. Shapaval and others (2013b) reported that the cultivation conditions (such as growth medium, growth temperature, and incubation time) affected the metabolic pathway of microorganisms, thereby triggering different biochemical compositions of the cells, which would have to be controlled and standardized strictly for their FTIR spectra. The authors attempted to differentiate 91 food spoilage yeast strains of 12 different genera by FTIR spectroscopy employing different cultivation media (YP, YPD, YMB, SAB, and SD). The radial basis function PLS model suggested that a YMB selective medium provided the best differentiation results for 9 of the 12 yeast genera with sensitivity above 90%. This information provided a competitively complementary approach for epidemiological studies.

Surface-Enhanced Raman Spectroscopy (SERS)

Different from the vibrational spectra obtained with IR absorption, Raman spectroscopy is based on scattering effects, which provide structural and chemical information of samples and permit the quantitative and qualitative analysis of individual compounds. When a sample is irradiated by monochromatic light with a frequency of ν_0, a portion of the irradiation is scattered. There are

2 types of light scattering: elastic and inelastic (Figure 1A). In the case of elastic scattering (also called Rayleigh scattering), the photon frequency or energy is the same as that of the incident light ($E = E_0$). Due to deactivation or excitation of molecular vibrations, the photon might gain (anti-Stokes Raman scattering) or lose part of the energy (Stokes Raman scattering) during inelastic scattering, leading to a shift in photon frequency (Das and Agrawal 2011). The difference in frequency is called Raman shift ($\Delta\nu$ in cm^{-1}), which relies on the molecular geometry and the chemical composition of the molecules responsible for scattering (Herrero 2008). Normally, functional groups such as –C–S–, –S–S–, –S–H–, –C═C–, –C═S–, and –N═N– provide stronger Raman signals when they exhibit more polarizability during the molecular vibration (Dijkstra and others 2005). Nonetheless, the Raman scattering intensity is always very low and the enhancement of Raman effects is often necessary for trace analysis (Lee and Herrman 2016).

The first SERS effect (Figure 1B) was observed by Fleischmann and others (1974) who found that the Raman signals of pyridine molecules adsorbed onto a roughened silver surface was orders of magnitude stronger than the "normal" Raman scattering. Since then, the SERS technology has developed rapidly due to advances in Raman instrumentation and nanofabrication. Two different enhancement mechanisms, known as electromagnetic and chemical enhancements, are widely accepted for explaining the SERS effect. Electromagnetic enhancement is the dominant mechanism which occurs when incident photons excite the electrons on the roughened noble metallic nanostructures, resulting in the localized surface plasmon resonance of the metal surface and inducing the electromagnetic field response for the formation of the SERS effect. On the other hand, chemical enhancement is another contributory factor causing various effects, including chemical interactions and charge-transfer between the molecule and nanoparticle, as well as the excitation of a higher electronic state of the molecule (Cialla and others 2012). Up to now, there are various noble metallic and semiconducting nanoparticles available for SERS substrates, which are normally fabricated into colloidal solutions, isolated nanostructures on a substrate, nanostructured films or electrodes, or arrays of coupled anisotropic nanostructures such as rhombus-like nanostructures, hexagonally arranged metallic nanotriangles, and coupled nanoparticle–nanowire systems (Sharma and others 2012).

SERS-based microorganism detection is generally classified into 2 approaches. One is direct detection of the intrinsic vibrational fingerprint of microorganisms, and the other is indirect detection using a SERS nanotag (such as QSY21) as a quantitative reporter. Recent applications of SERS and its combination with other separation or capturing technologies for detecting microorganisms are summarized in Table 1. As SERS is highly sensitive to many chemical components, for successful microorganism detection, the SERS spectra should be reproducible and reliable. Therefore, SERS-active nanostructures should be reproducible and should avoid any contamination from the environment and any interference from the microbial metabolites.

The metal colloid solution with nanoscale-size features is easily and cheaply prepared and has been widely used for SERS-active substrates. Researchers have successfully employed different metal substrates to detect a variety of microorganisms. Xie and others (2013) easily differentiated 7 foodborne pathogens of *Enterobacteriaceae* by Au-colloid based SERS coupled with PCA and HCA algorithms. David and others (2013) evaluated the ability for determining *Bacillus* bacterial spores using a portable spectrometer coupled with Ag colloidal substrates. In this study (David and others 2013), the dipicolinic acid was regarded as the biomarker of bacterial spores, and rapid quantification of dipicolinic acid at 5 ppb (29.9 nM) levels was achieved. This was obviously lower than the infective dose of 10^4 *B. anthracis* cells for inhalation anthrax. However, the method was limited by the dipicolinic acid extraction procedure from the spores.

In employing SERS-active substrates, the large variations in shape and size of nanoparticles, and the aggregation of colloidal metal nanoparticles are the main bottlenecks for improving the detection reproducibility. On the one hand, the introduction of stabilizers (for example, gelatin, polyvinyl alcohol, and polyvinyl pyrolidone) can control the metallic aggregation during the synthesis to transform metallic nanoparticles into stable solid substrates (Sundaram and others 2013). On the other hand, the substrates with highly uniform structures, such as the well-designed nanoparticle arrays, often give high sensitivity and reproducibility for SERS-sensing. Liu and others (2012) fabricated the Ag/AAO nanoparticle arrays substrate with Ag nanoparticle size and interparticle gaps about 30 nm and 10 nm, respectively, for the label-free and rapid detection of *Staphilococcus aureus*, *Klebsiella pneumoniae*, and *Mycobacterium smegmatis.* Their resultant substrate had a high reproducibility and exhibited almost 100% classification accuracy in these bacteria. In another study, Hennigan and others (2012) described a strategy using Ag nanorod array-based SERS for the direct detection of avian mycoplasmas, and their PLS-DA model resulted in sensitivity and specificity of above 93% for classifying different species of avian mycoplasmas. In addition, the quasi-3D (Q3D) Ag nanostructure arrays were built for strain-level detection and identification of *Vibrio parahaemolyticus* in situ (Xu and others 2013). However, when the bacterial concentrations were below 10^5 CFU/mL, the cells adhering to the substrate surface were too few to generate a measurable Raman signal.

In order to enable SERS for microorganism detection in real foodstuffs, it is necessary to develop some sample pretreatment approaches to separate or concentrate the microorganism from food matrices prior to SERS detection. These approaches mainly involve physical (such as centrifugation and filtration), chemical (such as lectins and dielectrophoresis), physicochemical (such as metal hydroxides), or biological approaches (such as immunomagnetic separation and bacteriophages) which can increase the microbial cellular adhesion ability to the substrate (Stevens and Jaykus 2004). Wu and others (2013) modified the Ag nanorod arrays substrates with a coating known as vancomycin, which could prevent the surface from reacting with unwanted substances, in order to capture 6 foodborne pathogens in mung bean sprouts. By combination with a two-step filtration process, this system could achieve foodborne pathogenic bacteria identification with a limit of detection (LOD) as low as 100 CFU/g mung bean sprouts within 4 h. Additionally, Wu and others (2015) also demonstrated the capability and advantages of their method to differentiate 27 bacterial isolates from 12 species with various strains and serotypes, and achieved 100% accuracy for the discrimination between Gram-positive and Gram-negative bacteria. The spectral features used for strain and serotype differentiation were mainly from adenine and the surface proteins, respectively. In another study, *Bacillus anthracis* spores in orange juice were rapidly captured and detected with LOD of 10^4 CFU/mL using an aptamer-functionalized Ag dendrites substrate (He and others 2013). In addition, Wang and others (2015) proposed a SERS biosensor consisting of a SERS substrate and a novel SERS tag for the detection of *Staphylococcus aureus* based on aptamer recognition. The Ag-coated magnetic

Table 1–Recent advances in microorganism detection by surface-enhanced Raman spectroscopy.

Microorganisms	Substrates and capturing techniques	Models	Results	References
Bacillus subtilis spores	Ag nanoparticle	/	1.5×10^9 spores/L	Cheng and others (2012)
Bacillus anthracis spores	Aptamer capture Ag dendrites	PCA	LOD of 10^4 CFU/mL in detection of spores in orange juice	He and others (2013)
Bacillus bacterial spores	Ag colloidal	PLSR, kernel PLSR	5 ppb DPA biomarker for Bacillus bacterial spores	Cowcher and others (2013)
Escherichia coli	Microfluidic chip Ag colloid	SVM	An accuracy of 92%	Walter and others (2011)
Escherichia coli	Biosynthesized Ag nanoparticles		LOD of 10^3 CFU/mL	Ankamwar and others (2016)
Escherichia coli	Immunoassay microarray flow through cells Ag colloid	/	Linear range between 4.3×10^3 to 4.3×10^5 cells/mL	Knauer and others (2012)
Escherichia coli	Immunomagnetic separation and filter membrane Ag intensification	/	Detection of about 10 CFU/mL for both pure culture and ground beef	Cho and others (2015)
Escherichia coli	Nano-immunomagnetic separation Au colloid	/	LOD of 10^2 CFU/mL in apple juice	Najafi and others (2014)
Escherichia coli	Microfluidic chip Iron oxide–gold core–shell nanoovals	/	LOD of 210 CFU/mL	Madiyar and others (2015)
Escherichia coli *Staphylococcus epidermidis*	Ag nanoparticles	/	2.5×10^2 cells/mL	Zhou and others (2014)
Escherichia coli *Salmonella enterica,*	Ag dendrites	PCA	LOD of 10^4 CFU/mL	Wang and others (2016c)
Escherichia coli *staphylococcus aureus*	Polyethylenimine-modified Au-coated magnetic microspheres Au@Ag nanoparticles	/	LOD of 10^4 CFU/mL	Wang and others (2016a)
Escherichia coli *Staphylococcus aureus* *Salmonella Typhimurium* *Listeria innocua*	Ag biopolymer nanoparticle	PCA, SIMCA	99% classification accuracy for PCA	Sundaram and others (2013)
Escherichia coli *Staphylococcus epidermidis, Enterococcus faecalis*	Intracellular nanosilver	PCA	Ability to reach the level of single cell	Fan and others (2011)
L. monocytogenes Scott A. Eight key foodborne pathogens	Microfluidic platform Ag colloid	PCA, LDA	LOD of 2 to 169 CFU/mL	Mungroo and others (2016)
Five avian mycoplasmas	Ag nanorod array	PLS-DA	>93% classification accuracy LOD of 100-fold greater than that of standard PCR and real-time quantitative PCR	Hennigan and others (2012)

(*Continued*)

Table 1–Continued.

Microorganisms	Substrates and capturing techniques	Models	Results	References
Klebsiella Pneumoniae *Mycobacterium smegmatis* *Staphilococcus aureus*	Ag/AAO nanoparticle Arrays	PCA, LDA, CA, SVM	Almost 100% classification accuracy	Liu and others (2012)
Salmonella enterica	4-mercaptophenylboronic acid functionalized Ag dendrites	//	LOD of 10^3 CFU/mL in 50 mM NH4HCO3 and 10^2 CFU/mL in both 1% casein and skimmed milk	Wang and others (2017c)
Salmonella typhimurium	Aptamerfunctionalized magnetic gold nanoparticles Aptamer and mercaptobenzoic acid functionalized Au nanoparticle	/	LOD of 5 CFU/mL	Ma and others (2016)
Salmonella typhimurium	Au@Ag core/shell nanoparticles (NPs) Aptamer capture	/	LOD of 15 CFU/mL	Duan and others (2016)
Salmonella typhimuriumStaphylococcus aureus	Fe_3O_4 magnetic Au nanoparticles Au nanoparticles Aptamer capture	/	The LOD is 35 CFU/mL for *S. aureus* and 15 CFU/mL for *S. typhimurium*	Zhang and others (2015)
Staphylococcus aureus	Incorporation of multilayered Ag nanoparticles into poly (oligo(ethylene glycol) methacrylate) brushes	/	LOD of 8 CFU/mL	Zhang and others (2017)
Staphylococcus aureus	Aptamer-modified Ag-coated magnetic nanoparticles	/	LOD of 10 cells/mL	Wang and others (2015)
Staphylococcus aureus	Microfluidics chip Ag colloid	PLSR	An average recognition rate of 95%, $R > 0.98$	Lu and others (2013)
Staphylococcus aureus	Au coated magnetic nanoparticles core/shell nanocomposites Antibody capture	/	LOD of 10 cells/mL	Wang and others (2016c)
Seven Enterobacteriaceae foodborne bacteria	Au colloid	PCA, HCA	Easy identification of bacteria	Xie and others (2012)
Six foodborne pathogenic bacteria	Vancomycin functionalized Ag nanorod arrays	PCA, PLS-DA	LOD of 100 CFU/mL in mung bean sprouts	Wu and others (2013)
Twenty-seven different bacteria isolates from 12 species	Vancomycin-coated Ag nanorod	PCA, HCA, PLS-DA	100% accuracy on distinguishing Gram-positive from Gram-negative bacteria	Wu and others (2015)
Vibrio parahaemolyticus	Fe_3O_4@Au particles wrapped with graphene oxide Aptamer capture	/	LOD of 14 CFU/mL	Duan and others (2017)
Vibrio parahaemolyticus	SiO_2@Au core/shell nanoparticles Aptamer capture	/	LOD of 10 CFU/mL	Duan and others (2016b)
Vibrio parahaemolyticus	Quasi-3D plasmonic nanostructure arrays	/	LOD ranging from 10^4 to 10^8 CFU/mL	Xu and others (2013)

Notes: AAO = anodic aluminum oxide, CA = clustering analysis, DPA = dipicolinic acid, HCA = hierarchical cluster analysis, LDA = linear discriminant analysis, LOD = limit of detection, PCA = principal component analysis, PLS-DA = partial least squares discriminant analysis, PLSR = partial least squares regression, SIMCA = soft independent modeling of class analogies, SVM = support vector machine.

nanoparticles substrate was modified by the aptamer, and the SERS tag was AuNR-DTNB@Ag-DTNB core-shell plasmonic nanoparticles or DTNB-labeled inside-and-outside plasmonic nanoparticles. This biosensor could achieve a LOD as low as 10 cells mL^{-1} for *S. aureus* detection, and it had a good linear relationship ranging from 10 to 10^5 cells/mL *S. aureus* concentration.

Immunomagnetic separation is an antibody-based isolation method that has been widely used for capturing the target microorganism from a complex food matrix directly. Najafi and others (2014) immobilized the capture antibodies (cAbs) on magnetic iron nanoparticles coated with gold nanoparticles (Fe_3O_4/Au substrate) for sensing *E. coli* O157 in apple juice. By eliminating sample preparation procedures, such as centrifugation and filtration, a capture efficiency of 84–94% and LOD of 10^2 CFU/mL for *E. coli* O157 in apple juice was achieved within 1 h. In addition, Cho and others (2015) combined the magnetic separation, membrane filtration, and silver intensification with SERS for the rapid detection of *E. coli* O157:H7 in ground beef, and an extremely low concentration of *E. coli* O157:H7 (about 10 CFU/mL) was identified within 3 h, showing a great potential for effectively routine monitoring of pathogens in foods.

Microfluidic platform is an emerging tool to conduct microfabrication for controlling and studying fluid behavior at the microscale. In recent years, the integration of microfluidics and SERS has drawn attention for its microorganism detection (Figure 2). For example, an immunoassay microarray flow-through system was developed by Knauer and others (2012). With this system, the *E. coli* bacteria were captured when they were pumped through the antibody spots inside the microarray chip channel, and the SERS-active Ag colloids were then brought in contact with the bound bacteria for SERS measurements. Recently, the nanotag-labeled *E. coli* DHα5 cells were effectively captured and concentrated with a nano-electrode array, which was integrated by embedding the vertically aligned carbon nanofibers to the bottom of a microfluidic chip (Madiyar and others 2015). This method yielded a LOD of 210 CFU/mL by a portable Raman probe, and the established system was reusable and amenable to field applications.

Terahertz time-domain spectroscopy

The terahertz (THz) radiation region occupies the electromagnetic spectrum from 0.1 to 10 THz (3.3 to 333.6 cm^{-1}), filling the frequency gap between microwave and far-IR regions. The THz gap remained unexplored until the advances during the 1980s in effective THz sources and detectors. THz radiation can excite the low-frequency biomolecular (such as protein and DNA) motions, including the vibration and rotation of the molecular skeleton from intra-molecular and inter-molecular modes connected by weak and conformation-related interactions such as hydrogen bonds, van der Waals force, and hydrophobic interactions (Wang and others 2017a). Thereby it is available for acquiring unique structural and dynamic information that is absent in other electromagnetic spectroscopies (Yang and others 2016b). With the technological innovation in optics and electronics, THz-based spectroscopic sensing and imaging techniques have developed rapidly, especially for the THz-TDS, which has been widely utilized in security screening, biomedical research, and food quality evaluations (Park and others 2014a).

Different from infrared and Raman spectroscopies, by which only the intensity of light at specific frequencies can be obtained, both the amplitude and the phase of the THz waves are measured using THz-TDS, and both the absorption coefficient and the refractive index of samples can thus be evaluated (Mantsch and Naumann 2010). The exploration of THz spectral fingerprints can complement the knowledge of spectral data obtained from IR and Raman spectroscopy for microbial detection. Furthermore, the detection of biological tissue samples with THz radiation is not easily affected by scattering due to its longer wavelengths. More attractively, THz waves can pass through many commonly used nonpolar dielectric materials such as plastic, clothing, cardboard, paper, masonry, textiles, and ceramics with little attenuation. Moreover, its minimal radiation photon energy compared with X-ray radiation would not lead to light ionization or bio-molecule damage (Ok and others 2014). Consequently, THz-TDS is suitable for noninvasive sensing targets under covers in containers.

The detection of microorganisms in the THz frequency range has generated interest. Microorganisms are complex biological objects. When THz waves excite the microbial cells, their cellular components can contribute to low-frequency biomolecular motions and result in specific THz spectroscopic features. This is critical for microbial spores and cell detection, as well as for monitoring the changes in cellular components (Globus and others 2012). In addition, Globus and others (2012) demonstrated the capability of THz-TDS for the rapid estimate of the living state of *Escherichia coli* and *Bacillus subtilis*. On the other hand, Yang and others (2016a) recently assessed the living state of bacteria from the same species, and they reported that the small differences in hydration levels between bacterial cells was another crucial reason accounting for the different absorption coefficients of THz spectra, which allowed for the bacterial species identification and classification. Furthermore, THz-TDS also shows the potential for detecting unknown bacteria after the establishment of the microbial THz spectral reference databases, which consist of the absorption coefficients delineated by their hydration levels.

However, microorganisms are transparent in the THz frequency range and the sizes of typical microorganisms are often extremely smaller than the THz wavelength (λ) (in the order of $\sim\lambda/100$). Such a size mismatch normally results in a low scattering cross-section, thus hindering the sensitivity of the measurement of microbial cells with small quantities (Park and others 2014b). In some cases, THz antennas and metamaterials could generate strong localized and enhanced fields, which enable the sensitive measurement of a small number of chemical and biological substances by studying the frequency shift of resonances (Park and others 2014a). The resonance frequency shift of metamaterials deposited with microorganisms is normally associated with the dielectric constant and the density of the microorganism within a gap area.

Kurita and others (2014) used a metallic mesh sensor, which can measure the dielectric property of a material, to specifically detect *E. coli* in THz region. Anti-*E.coli* antibodies were immobilized on the metallic mesh surface for capturing the *E. coli*. Kurita and others (2014) demonstrated that there was a significant relationship between the THz frequency shift and the concentration of *E. coli,* which could be used for the quantitative measurement of *E. coli* concentration. However, the high LOD of 10^6 CFU/mL was unsatisfactory and thus further studies are required. Park and others (2014a) fabricated a metamaterial sensor that is an array of a square ring with a micro-gap at the center for the highly sensitive, high-speed, and on-site detection of microorganisms (Figure 3). Extremely small amounts of microorganisms including bacteria, molds, and yeasts were detected in both ambient and aqueous environments by the THz metamaterial. Additionally, selective detection would be possible when the substrates were functionalized with specific antibodies to the target microorganism. In another study, silicon-based THz bowtie antennas were

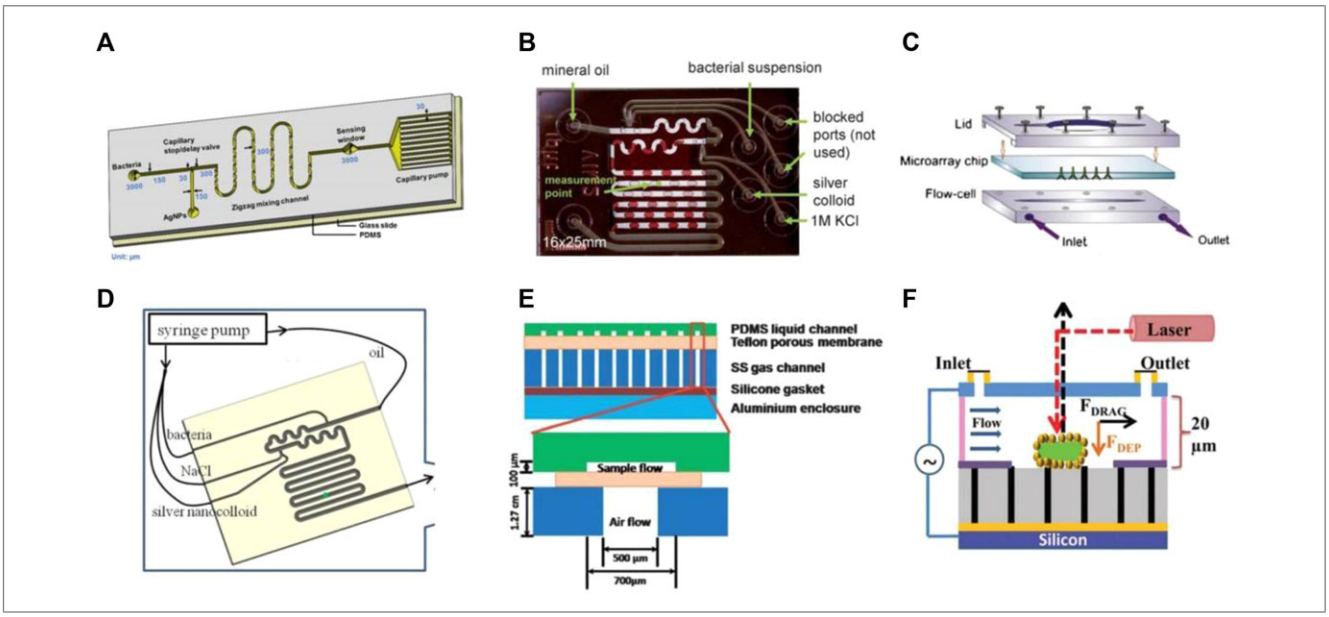

Figure 2–Representative SERS-microfluidic systems for microorganism detection. (A) a microfluidic chip consisted of 2 inlets and 1 outlet connected with a capillary pump (Mungroo and others 2016); (B) a microfluidic chip with 6 injection ports (Walter and others 2011); (C) an immunoassay microfluidic system (Knauer and others 2012); (D) an automated PDMS-based optofluidic platform (Lu and others 2013); (E) 2-layered design of the evaporation microfluidics (Zhang and others 2010); (F) a microfluidic dielectrophoresis device in a "point-and-lid" geometry (Madiyar and others 2015).

prepared by Berrier and others (2012), who selectively identified the Gram-negative type within the 5 different bacteria that most likely arose from the structural and chemical differences in the cell. In conjunction with chemometric methods, Berrier and others (2012) demonstrated that the proposed technique could be employed to determine the Gram positive or negative type of an unknown sample, and thus it might be useful as a rapid antibiotic efficacy test.

Recently, the THz antenna and the metamaterial sensor fabricated on low-dielectric constant substrates (quartz and flexible polyimide film) were demonstrated to have higher sensitivity for microorganism detection than that fabricated on a high-dielectric constant substrate (silicon) (Park and others 2014b; Tenggara and others 2017). The substrate with small thickness also performed at higher sensitivity due to its effective dielectric constant, which offered another valuable opportunity for building a THz sensor with high sensitivity. Mazhorova and others (2012) proposed a suspended-core THz fiber sensor for *E. coli* detection based on the evanescent field effect. In their study, T4 bacteriophages were bio-functionalized with the fiber core for binding and eventually destroying their target bacteria, which unambiguously resulted in a strong increase of the fiber absorption. Therefore, *E. coli* was effectively measured with a LOD of 10^4 CFU/mL that need not depend on the microbial "fingerprint" features in the THz spectrum.

Laser induced breakdown spectroscopy (LIBS)

LIBS is a relatively new and versatile spectroscopic technique for in situ elemental detection and quantitative chemical analysis based on atomic emission spectroscopy. The basic principle of LIBS technique is employing a pulsed focused laser and a focusing lens to generate the plasma which vaporizes a small amount of samples; a spectrometer is used to collect the plasma light that consists of vaporized atoms, ions, electrons, and molecular fragments, and then a detector is used to record the emission signals (Spizzichino and Fantoni 2014). By monitoring the emission line positions and intensities, qualitative and quantitative analyses are available. This technology does not require the target sample to be Raman- or infrared-active, and it is considered as the only spectroscopy that can give distinct special signature features of all chemical species in all environments (Miziolek and others 2006). Therefore, LIBS technique provides several strengths over the conventional elemental analysis methods. Because the plasma is produced by optical radiation, the LIBS approach is able to analyze different types of samples, including solid, liquid, and gas states, and it is particularly useful for analyzing a complex matrix directly. More importantly, this technique only needs a very small amount of sample, requires minimal sample preparation, and the results are available rapidly (seconds to minutes) (Harmon and others, 2013).

In the last 3 decades, with the striking technological innovations in the lasers, spectrographs, and detectors, LIBS technique has been aggressively investigated in the field of biological, medical, nanotechnology applications and for food quality control. In the case of microorganism detection, research studies on LIBS technology mainly focus on bacterial identification and differentiation since the initial demonstration in 2003. After that, many multivariate chemometric analyses are employed to classify bacterial LIBS spectra. The neural networks algorithm combined with LIBS spectra was demonstrated as a favorable method to identify and differentiate specific bacterial species (*Pseudomonas aeroginosa, Escherichia coli, Salmonella typhimurium, and the mold genus Candida*) with high accuracy (Marcos-Martinez and others 2011; Manzoor and others 2014; Manzoor and others 2016). In addition, Putnam and others (2015) compared different variable selection strategies and multivariate analysis techniques for LBIS bacterial classification. They found that a model composed of 80 independent variables provided the greatest sensitivity and specificity. Although the 2 multivariate techniques, discriminant function analysis and PLS-DA, both provide effective classification of unknown bacterial LIBS spectra, PLS-DA performed more precise to identify

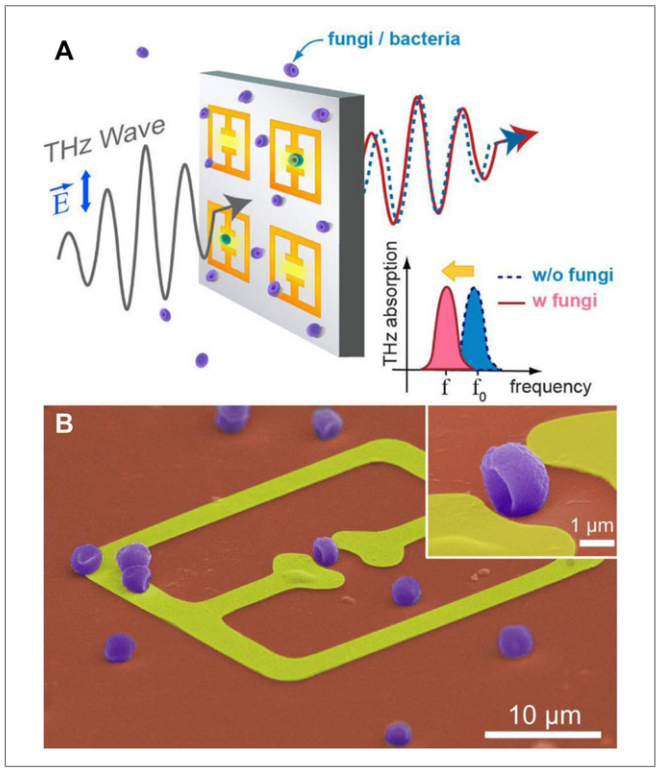

Figure 3–A typical microorganism-sensing using THz metamaterials. (A) A schematic presentation of THz metamaterials-sensing of microorganisms. (B) A color-enhanced SEM image of metamaterials coated by penicillia (Park and others 2014a).

the bacteria at the species-level or strain-level. To differentiate the microorganism by LIBS, the sample preparation is also a critical procedure. Gamble and others (2016) reported that both pH and the mineral cations of the water source used in purification of the culture must be taken into account. In addition to differentiate bacterial species, the metabolic state (live and dead) of *Escherichia coli* also can be detected based on LIBS spectral emission intensities of key elements, including Mg, P, K, Na, and Ca (Sivakumar and others). Also, Multari and others (2013) reported that the multivariate regression analysis of LIBS data is an ideal method to differentiate the live bacterial pathogens *E. coli* O157:H7 and *S. enterica* on various foods, including ground beef, lettuce, eggshell, milk, bologna, and chicken. And yet, despite the LBIS possesses the advantages of rapid and minimal sample preparation, Barnett and others (2012) suggested that LBIS might be limited for the quantitative detection of *Salmonella enterica* serovar Typhimurium in real food (milk, chicken broth, and brain heart infusion) due to its less sensitivity. Therefore, future works should be focused on improving the sensitivity and specificity of the LIBS system for the detection various pathogenic microorganisms.

Spectral Imaging Techniques

Hyperspectral imaging (HIS)

HSI, also known as imaging spectrometry, integrates both imaging or computer vision (Sun and Brosnan 2003; Sun 2004; Du and Sun 2005; Jackman and others 2009; Jackman and others 2011; Xu and Sun 2017; Xu and others 2017) and spectroscopic techniques into 1 system. In comparison with routine imaging or spectroscopic techniques, HSI can measure both spatial information and spectral parameters for each pixel in the image simultaneously (ElMasry and others 2012). A hyperspectral image, expressed as a hypercube I (x, y, λ), is a 3-dimensional (3D) block of data containing 1 wavelength λ and 2 spatial (x, y) dimensions. It can be considered either as a spectrum I (λ) at each individual pixel (x, y), or as an image I (x, y) at each individual wavelength λ (Cheng and others 2017). Each position within the specimen displays a unique spectral fingerprint of that pixel, which can be used to characterize its chemical component. As such, hyperspectral imaging can be used for the identification and the quantification of chemical compositions as well as the visualization of their distribution simultaneously (Wu and Sun 2013; Ravikanth and others 2017).

In terms of HSI, several systems including visible (Vis), near-IR, FTIR, fluorescence, as well as Raman HSI are available, which have great flexibility and offer multi-choices for inspecting diverse food products (Gowen and others 2015). Among them, visible and near-infrared (Vis-NIR) HSI is the most widely used system for assessment (ElMasry and others 2013; Cheng and Sun 2015; Cheng and others 2015; Cheng and others 2015; Pu and others 2015; Pu and others 2015; Xiong and others 2015; Cheng and others 2016; Cheng and others 2016; Dai and others 2016; Ma and others 2016; Pu and others 2016; Xu and others 2016; Cheng and Sun 2017; Cheng and Sun 2017; Li and others 2017).

Depending on the relative arrangement between the illumination system and the optical detector, HSI is commonly based on 3 types of sensing modes, namely, reflectance, transmittance, and interactance (ElMasry and others 2012). The hypercube I (x, y, λ) can be acquired by point-scanning, line-scanning, area-scanning, and single-shot approaches (Wu and Sun 2013). HSI was initially established for remote sensing applications, but it has been available for application in such diverse fields as medicine, pharmaceuticals, and food science. In terms of agro-food inspection, researchers have employed hyperspectral images to detect and quantify microorganism distribution in real samples (Siripatrawan and others 2011).

The principle underlying HSI for microorganism detection is based on the assumption of metabolites that can provide characteristic fingerprints to indicate the contamination of microorganisms in food matrices (Siripatrawan and others 2011). Similar to IRS analysis, the collected HSI data are often combined with various chemometrics to build the prediction models. In order to enhance the model performance, preprocessing and wavelength selection schemes are crucial. Therefore, Vis-NIR HSI has been applied to evaluate microbial infection in vegetable and meat products. Table 2 summarizes recent advances in microorganism detection.

Siripatrawan and others (2011) assessed *E. coli* contamination in packaged fresh spinach by HSI ranging from 400–1000 nm. Reflectance spectra were obtained and combined with PCA and ANN to predict the number of *E. coli* with R^2 of 0.97. ANN was used to construct a prediction map that visualized spatial information of *E. coli* contamination. For meat and meat products, highly perishable due to moist and nutritious surfaces suitable for bacteria growth, reliable and rapid detection of microorganism contamination is necessary. Tao and others (2012) collected the scatter images of *E. coli*-contaminated pork and then fitted them by Lorentzian distribution function, giving 3 parameters, namely a (asymptotic value), b (peak value), and c (full width at b/2). Afterwards, multiple linear regression (MLR) models were developed based on the parameters of a and "a&b&c" for predicting *E. coli* contamination, these were validated with good performance having R_{CV} of 0.877 and 0.841, respectively.

Table 2–Recent advances in microorganism detection by hyperspectral and multispectral imaging.

Techniques	Samples	Microorganisms	Spectral range (nm)	Models	R or R^2	References
HSI	Beef	TVC	400 to 1100	MLR	0.95	Peng and others (2011)
	Chicken	TVC	910 to 1700	PLSR, stepwise regression	0.97	Feng and Sun (2013a)
	Chicken	Enterobacteriaceae	930 to 1450	PLSR	0.89	Feng and others (2013)
	Chicken	Pseudomonas	900 to 1700	SNV-PLSR	>0.81	Feng and Sun (2013b)
	Grass carp fish	TVC	400 to 1000	PLSR	0.93	Cheng and Sun (2015a)
	Grass carp fish	*E. coli*	400 to 1000	PLSR, MLR	0.880 and 0.860	Cheng and Sun (2015b)
	Farmed salmon	Lactic acid bacteria	900 to 1700	LS-SVM	0.929	He and others (2014)
	Pork meat	TVC	400 to 1100	SMLR	0.94	Tao and Peng (2015)
	Pork meat	TVC	430 to 960	SI-PLS, PCA	0.8038	Huang and others (2013)
	Pork meat	TVC, PPC	900 to 1700	PLSR	0.86 and 0.89	Barbin and others (2013)
	Pork meat	*E. coli*	400 to 1100	MLR	0.877	Tao and others (2012)
	Mushrooms	*Pseudomonas tolaasii*	400 to 1000	PLS-DA	0.95	Gaston and others (2011)
	Spinach	*E. coli*	400 to 1000	PCA, ANN	0.97	Siripatrawan and others (2011)
	/	*Fusarium*	1000 to 2498	PCA, PLS-DA	/	Williams and others (2012)
	/	Five foodborne bacteria	900 to 2500	PCA, PLS-DA	0.82 to 0.99	Kammies and others (2016)
	/	*Salmonella*, Staphylococcus	450 to 800	SVM	0.999	Park and others (2015)
	/	*E. coli*	368 to 1024	PCA, kNN	0.97	Yoon and others (2013)
MSI	Beef	TVC	18 different wavelengths ranging from 405 to 970	PLS-DA, PLSR	0.90 to 0.93	Panagou and others (2014)
		Pseudomonas spp. *Brochothrix thermosphacta*				
	Cooked pork sausages	APC	405,435, 450, 470, 505, 525, 570, 590, 630, 645, 660, 700, 780, 850, 870, 890, 910, 940, 970	PLSR	0.89	Ma and others (2014)
	Pork meat	TVC	405, 435, 450, 470, 505, 525, 570, 590, 630, 645, 660, 700, 850, 870, 890, 910, 940, 970	PLSR	0.80	Dissing and others (2013)

Notes: HSI = hyperspectral imaging, TVC = total viable count, PLSR = partial least squares regression, MLR = multiple linear regression, SMLR = stepwise multiple linear regression, SI-PLS = Synergy interval partial least squares, PCA = principal component analysis, PPC = psychrotrophic plate count, LS-SVM = least squares support vector machine, ANN = artificial neural network, PLS-DA = partial least squares discriminant analysis, SVM = support vector machine, kNN = k-nearest neighbor classification, MSI = multispectral imaging, APC = aerobic plate count.

In many cases, although the prediction models with full wavelengths can give a good performance in the assessment of microorganisms, the data processing efficiency would be limited due to the large number of wavelengths involved in the calibration. Therefore, it is important to select the most informative wavelengths (MIWs) that are most relevant to microorganism prediction across the whole wavelength range by employing algorithms (such as stepwise regression, genetic algorithm, and successive projections algorithm). Many studies indicated that the predictions established on MIWs could also give satisfactory results for evaluating *Enterobacteriaceae* (Feng and others 2013; Cheng and Sun 2015b), *Pseudomonas* (Feng and Sun 2013b), and lactic acid bacteria (He and others 2014) in contaminated meat products.

The total viable count (TVC) of bacteria is a useful indicator for assessing the contamination extent of food products. When the TVC of bacteria exceeds a certain limit, it indicates that the food may be dangerous and may cause health problems owing to the generation of toxic compounds in the food or in its eater. In recent years, the application of HSI in different spectral collection modes, including reflectance, absorbance, scattering, and light diffuse reflectance, to assess the TVC in pork (Huang and others 2013; Tao and Peng 2015), chicken (Feng and Sun 2013a), beef (Peng and others 2011), and fish (Cheng and Sun 2015a) have been investigated. A typical TVC detection using HSI technology is shown in Figure 4. In addition, psychrotrophic bacteria can grow at low temperatures, and they are regarded as emblematic spoiling organisms of various chilled meats. Barbin and others (2013) measured the TVC and psychrotrophic plate count (PPC) in chilled pork during storage by HSI in the near-IR range. The PLSR models gave good prediction with R^2 of 0.86 and 0.89 for log (TVC) and log (PPC), respectively. The results suggested that HSI technology has promising potential for rapid, nondestructive, and reliable evaluation of microbial presence in meat.

Besides quantitative analysis of the number of microorganisms in food matrices, the potential for the differentiation and the classification of microorganisms by HSI technology have also been demonstrated. For example, 3 *Fusarium* species (*Fusarium subglutinans, Fusarium proliferatum,* and *Fusarium verticillioides*) inoculated on potato dextrose agar could be differentiated with reasonable accuracy based on HSI and PCA analysis (Williams and others 2012). Also, Yoon and others (2013) rapidly identified colonies of the big-6 non-O157 shiga-toxin-producing *E. coli* serogroups on rainbow agar plates by HSI at wavelengths ranging from 750 to 1000 nm. The classification accuracy based on the k-nearest neighbor classification (kNN, k = 3) was 95% at pixel level and 97% at colony level. In another study, Park and others (2015) analyzed the scattering intensity of spectral images from various Gram-negative and Gram-positive pathogenic bacteria by an acousto-optic tunable filter (AOTF)-based hyperspectral microscope imaging, and they found that a classification accuracy of 99.99% and kappa coefficient of 0.9998 were achieved by combining the scattering intensity data and SVM analysis. Recently, pathogenic and nonpathogenic bacteria and similar species of the same genera were also differentiated by Vis-NIR HSI (Kammies and others 2016). All the foregoing studies confirm that the detection and the discrimination of microorganisms to specific bacterial genera/groups can provide more insights to better understand the ecology of bacteria, thereby providing effective approaches for food safety control. However, most of the studies were focused on microorganisms inoculated on agar plates. Therefore, future work should consider using the HSI technique to classify microorganisms contaminating real food matrices.

Multispectral imaging (MSI)

MSI is another spectral imaging technology based on HSI technology. As aforementioned, the HSI technique provides a 3D hypercube that contains rich spatial information in full wavebands, which leads to difficulties in data processing, thus causing awkwardness in industrial online applications. In order to overcome this drawback, a simplified version known as MSI is available. There are some similarities between MSI and HSI techniques. For instance, both of them can gain the spatial and spectral information simultaneously in the form of a 3D hypercube, and the data acquisition process is nondestructive. The distinctive difference between these 2 methods depend mainly on the number of spectral bands involved in the hypercube. In general, there are more than 100 contiguous and regular spectral bands in the case of HSI, whereas normally only fewer than 20 noncontiguous and irregularly spectral bands are relevant to the food quality and safety evaluation for MSI. It should be noted that the feature wavelengths for MSI online analysis are commonly selected by a HSI system. Consequently, the robustness of HSI models for selecting feature wavelengths will significantly influence the successful application of a MSI system (Pu and others 2015). Although MSI systems cannot provide fine details in the spectral signatures in every image pixel from the objects, in general, the instrumental complexity and cost, as well as data acquisition time of MSI systems, are significantly lower than those of HSI systems. Recently, MSI systems combined with chemometrics have been employed for microorganism detection in meat products, and the main steps are shown in Figure 5.

Dissing and others (2013) assessed the spoilage degree in pork meat based on the prediction of TVC using MSI. They classified the pork meats stored at temperatures of 0, 5, 10, 15, and 20 °C and packaged in aerobic and modified atmosphere conditions into 3 categories of fresh, semi-fresh, and spoiled. The multispectral images acquired at 18 unregularly distributed wavelengths (405, 435, 450, 470, 505, 525, 570, 590, 630, 645, 660, 700, 850, 870, 890, 910, 940, and 970 nm) in conjunction with various chemometrics were employed to predict the quality of these meats. For the microbial counts, a good predictive result with overall classification performance of 80.0% was achieved, providing a promising approach for evaluating pork spoilage. Panagou and others (2014) assessed the potential of MSI for the rapid and nondestructive determination of the microbiological quality of beef fillets during aerobic storage at refrigerated and abuse temperatures. A PLS-DA model was established for the classification of beef fillets with different spoilage degrees, achieving an overall correct discrimination rate of 91.8% and 80.0% for model calibration and validation, respectively. In addition, based on the developed PLSR models, the quantitative estimation of TVC, *Pseudomonas spp.*, and *Brochothrix thermosphacta* showed regression coefficients ranging from 0.90 to 0.93 (Panagou and others 2014). In another study, Ma and others (2014) estimated aerobic plate count (APC) numbers in cooked pork sausages by combining the MSI technique with PLSR analysis, presenting a good result with R^2 of 0.89. All these studies demonstrate that the MSI technique has the potential to be an alternative and promising approach for practical and industrial online applications.

Challenges and Future Outlook

Spectroscopic and spectral imaging techniques, along with the advantages of rapid, nondestructive, label-free, in situ, or on-line detection, are attractive and competitive for the food industry. Nonetheless, foodstuffs are heterogeneous in nature, thereby some

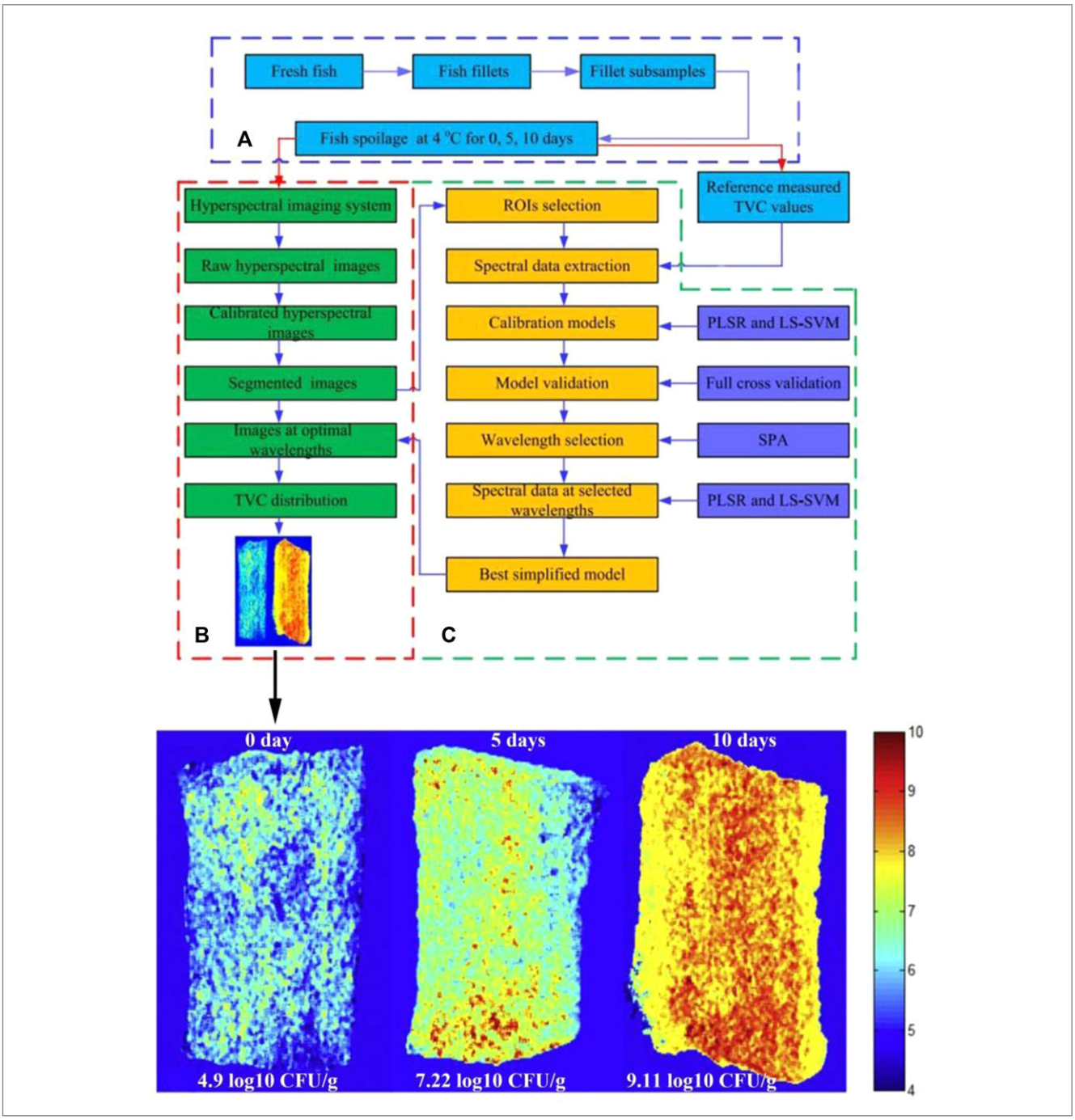

Figure 4–Main steps of microorganism determination in meat products by HSI technique (Cheng and Sun 2015a).

challenges remain to be resolved for microorganism detection in food matrices.

A primary challenge for spectroscopic and spectral imaging techniques relates to their complex fingerprints. Therefore, extensive data pretreatments and appropriate chemometrics are often required to build reliable and robust prediction models. The microorganism reference databases built by spectral pretreatment and multivariate analysis should have sufficient generality. However, this is difficult due to the high intraspecies phenotypic biodiversity of microorganisms, which makes the building of a worldwide accessible reference database a challenge. Furthermore, the existence of significant redundant data in hyperspectral images poses a challenge for data mining and data processing. The complexity and high cost of the instruments needs to be considered. SERS is highly sensitive to fingerprints that are often characteristic of analytes, rendering it attractive for measuring microorganisms in complex matrices. However, biological fluorescence will result in an interfering background, limiting the practical applications of SERS in the food industry. In addition, improving the reproducibility of substrates for SERS analysis is also a challenge. With respect to THz-TDS, the absorption by water, as well as the size mismatch between the microbial

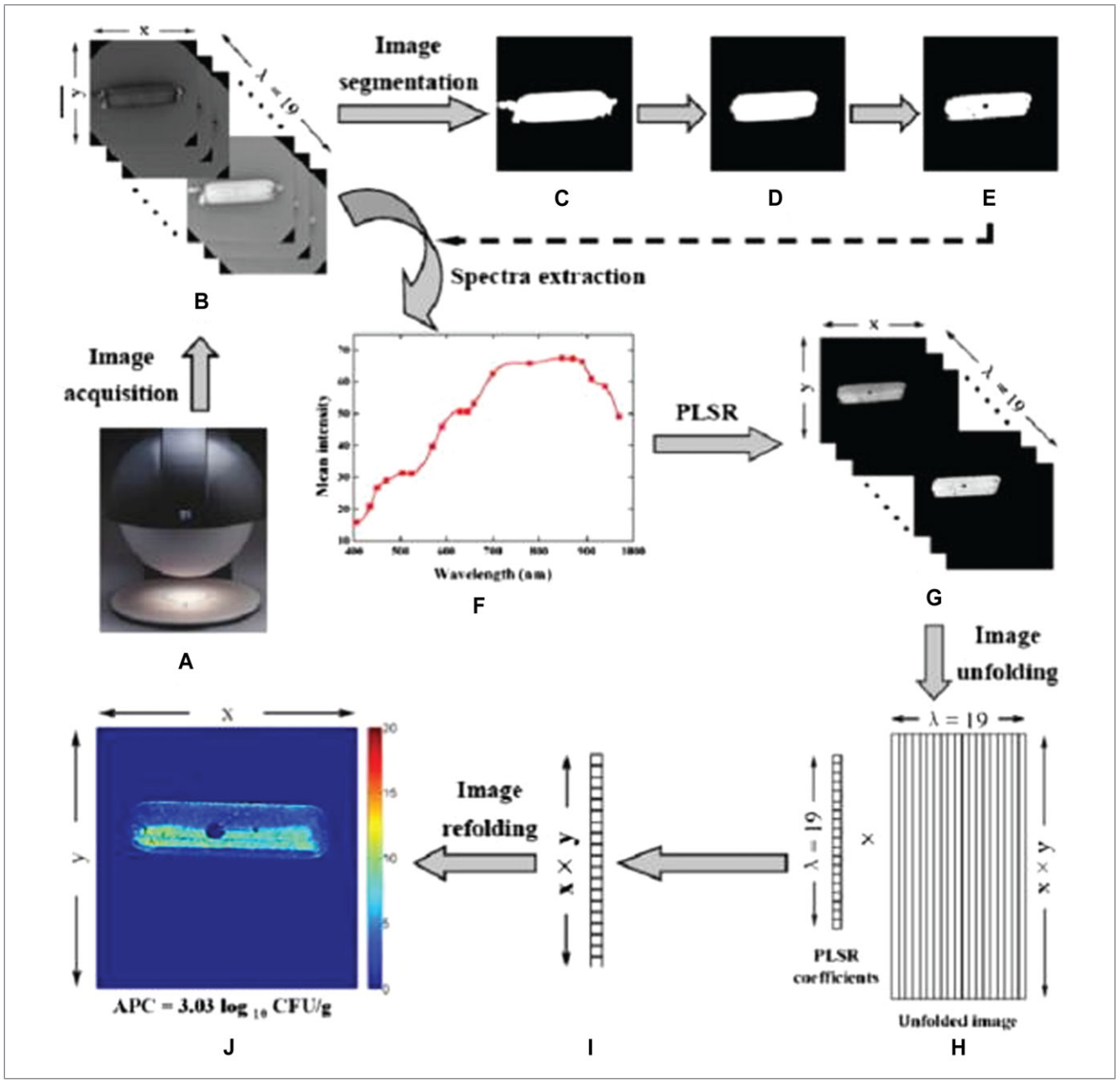

Figure 5–Main steps involved in application of MSI technology and chemometrics to obtain the contamination map of microorganisms in meat products (Ma and others 2014).

cells and terahertz wavelength, can hamper the sensitivity for microorganism detection. The major challenge of LIBS results from its low sensitivity for the minor mineral elements analysis in microorganisms.

In the future, more effective algorithms should be used for spectral data processing and microorganism reference database building. Employing new algorithms to select informative wavelengths across the whole wavelength range is important for implementing MSI systems, which are more efficient, inexpensive, and suitable for on-line detection of microorganisms. In the case of SERS and THz-TDS techniques, attention should be given to couple the SERS substrates and THz antennas or metamaterials with a microfluidic platform. By integrating with capture approaches, such as antibodies and aptamers on the lab-on-a-chip device, the resultant sensors should be able to reduce the interference from food matrices and provide the selective and sensitive detection of the target microorganism in situ. In addition, the incorporation of the ATR technique into the THz-TDS would significantly eliminate interference from moisture, and the combination of LIBS with other spectroscopic (such as laser-induced Raman and fluorescence) techniques can unite the features of them. The research into microbial quantification and discrimination, as well as studies on microbial cellular modification in response to food-processing stress, by spectroscopic and spectral imaging technologies will also be of interest in the future. Finally, the acceleration of developing portable spectroscopic and imaging systems with simplicity and reliability should facilitate early adoption of these technologies in the food industry.

Conclusions

The principles and recent advances of spectroscopic and spectral imaging techniques, including IRS, SERS, THz-TDS, LIBS, HSI, and MSI, are summarized in this review. In general, spectroscopic and spectral imaging techniques can achieve rapid, nondestructive, or label-free detection, rendering them attractive for routine microorganism detection in the food industry. However, there also some challenges for realizing this goal. With the development in instruments and algorithms, as well as the integration of microfluidic platforms, the spectroscopic and spectral imaging techniques will provide alternative methods for microorganism detection in the future.

Acknowledgments

The authors are grateful to the International S&T Cooperation Program of China (2015DFA71150) for its support. This research was also supported by the Collaborative Innovation Major Special Projects of Guangzhou City (201508020097, 201604020007, 201604020057), the Guangdong Provincial Science and Technology Plan Projects (2015A020209016, 2016A040403040), the Key Projects of Administration of Ocean and Fisheries of Guangdong Province (A201401C04), the National Key Technologies R&D Program (2015BAD19B03), the International and Hong Kong - Macau - Taiwan Collaborative Innovation Platform of Guangdong Province on Intelligent Food Quality Control and Process Technology & Equipment (2015KGJHZ001), the Guangdong Provincial R & D Centre for the Modern Agricultural Industry on Nondestructive Detection and Intensive Processing of Agricultural Products, the Common Technical Innovation Team of Guangdong Province on Preservation and Logistics of Agricultural Products (2016LM2154) and the Innovation Centre of Guangdong Province for Modern Agricultural Science and Technology on Intelligent Sensing and Precision Control of Agricultural Product Qualities. In addition, the authors wish to acknowledge the contribution of Paul B McNulty, Emeritus Professor of Biosystems Engineering, University College Dublin, Ireland, who assisted in editing this manuscript.

Nomenclature

AAO	Anodic aluminum oxide
ANN	Artificial neural network
APC	Aerobic plate count
BP-ANN	Back-propagation artificial neural network
CA	Clustering analysis
CVA	Canonical variate analysis
DA	Discriminant analysis
FTIR	Fourier transform infrared
GA	Genetic algorithm
HCA	Hierarchical cluster analysis
HSI	Hyperspectral imaging
IRS	Infrared spectroscopy
kNN	k-nearest neighbor classification
LDA	Linear discriminant analysis
LIBS	Laser-induced breakdown spectroscopy
LOD	Limit of detection
LS-SVM	Least squares support vector machine
MLR	Multiple linear regression
MSI	Multispectral imaging
MIWs	Most informative wavelengths
PCA	Principal component analysis
PLS	Partial least squares
PLSR	Partial least squares regression
PPC	Psychrotrophic plate count
RF	Random forest
SERS	Surface-enhanced Raman spectroscopy
SI-PLS	Synergy interval partial least squares
SIMCA	Soft independent modeling of class analogies
SMLR	Stepwise multiple linear regression
SVM	Support vector machine
THz-TDS	Terahertz time-domain spectroscopy
TVC	Total viable count

References

Alexandrakis D, Downey G, Scannell AG. 2011. Detection and identification of selected bacteria, inoculated on chicken breast, using near infrared spectroscopy and chemometrics. Sens Instrum Food Qual Saf 5:57–62.

Alvarez-Ordonez A, Mouwen D, Lopez M, Prieto M. 2011. Fourier transform infrared spectroscopy as a tool to characterize molecular composition and stress response in foodborne pathogenic bacteria. J Microbiol Meth 84:369–78.

Ankamwar B, Sur UK, Das P. 2016. SERS study of bacteria using biosynthesized silver nanoparticles as the SERS substrate. Anal Methods-UK 8:2335–40.

Barbin DF, ElMasry G, Sun D-W, Allen P, Morsy N. 2013. Nondestructive assessment of microbial contamination in porcine meat using NIR hyperspectral imaging. Innov Food Sci Emerg 17:180–91.

Barnett C, Bell C, Vig K, Akpovo AC, Johnson L, Pillai S, Singh S. 2011. Development of a LIBS assay for the detection of *Salmonella enterica* serovar Typhimurium from food. Anal Bioanal Chem 400:3323–30.

Berrier A, Schaafsma MC, Nonglaton G, Bergquist J, Rivas JG. 2012. Selective detection of bacterial layers with terahertz plasmonic antennas. Biomed Opt Express 3:2937–49.

Calvo J, Calvente V, Orellano ME, Benuzzi D, Sanz MI. 2010. Control of Penicillium expansum and Botrytis cinerea on apple fruit by mixtures of bacteria and yeast. Food Bioprocess Tech 3(5):644-50.

Chen CY, Nace GW, Irwin PL. 2003. A 6× 6 drop plate method for simultaneous colony counting and MPN enumeration of *Campylobacter jejuni*, *Listeria monocytogenes*, and *Escherichia coli*. J Microbiol Meth 55:475–9.

Cheng HW, Huan SY, Yu RQ. 2012. Nanoparticle-based substrates for surface-enhanced Raman scattering detection of bacterial spores. Analyst 137:3601–8.

Cheng JH, Nicolai B, Sun D-W. 2017. Hyperspectral imaging with multivariate analysis for technological parameters prediction and classification of muscle foods: A review. Meat Sci 123:182–91.

Cheng JH, Sun D-W. 2015. Rapid and non-invasive detection of fish microbial spoilage by visible and near infrared hyperspectral imaging and multivariate analysis. LWT-Food Science and Technology 62:1060–8.

Cheng JH, Sun D-W. 2015a. Rapid and non-invasive detection of fish microbial spoilage by visible and near-infrared hyperspectral imaging and multivariate analysis. LWT-Food Sci Technol 62:1060–8.

Cheng JH, Sun D-W. 2015b. Rapid quantification analysis and visualization of *Escherichia coli* loads in grass carp fish flesh by hyperspectral imaging method. Food Bioprocess Tech 8:951–9.

Cheng J-H, Sun D-W, Pu H. 2016. Combining the genetic algorithm and successive projection algorithm for the selection of feature wavelengths to evaluate exudative characteristics in frozen-thawed fish muscle. Food Chemistry 197:855–63.

Cheng J-H, Sun D-W, Pu H, Zhu Z. 2015. Development of hyperspectral imaging coupled with chemometric analysis to monitor K value for evaluation of chemical spoilage in fish fillets. Food Chemistry 185:245–53.

Cheng L, Sun D-W, Zhu Z, Zhang Z. 2017. Emerging techniques for assisting and accelerating food freezing processes: A review of recent research progresses. Critical Reviews in Food Science and Nutrition 57:769–81.

Cheng J-H, Sun D-W, Qu J-H, Pu H-B, Zhang X-C, Song Z, Chen X, Zhang H. 2016. Developing a multispectral imaging for simultaneous prediction of freshness indicators during chemical spoilage of grass carp fish fillet. Journal of Food Engineering 182:9–17.

Cheng J-H, Sun D-W. 2017. Partial least squares regression (PLSR) applied to NIR and HSI spectral data modeling to predict chemical properties of fish muscle. Food Engineering Reviews 9:36–49.

Cheng J-H, Sun D-W, Pu H-B, Wang Q-J, Chen Y-N. 2015. Suitability of hyperspectral imaging for rapid evaluation of thiobarbituric acid (TBA)

value in grass carp (Ctenopharyngodon idella) fillet. Food Chemistry 171:258–65.

Cheng W, Sun D-W, Cheng J-H. 2016. Pork biogenic amine index (BAI) determination based on chemometric analysis of hyperspectral imaging data. LWT-Food Science and Technology 73:13–9.

Cheng J-H, Sun D-W. 2017. Partial least squares regression (PLSR) applied to NIR and HSI spectral data modeling to predict chemical properties of fish muscle. Food Engineering Reviews 9:36–49.

Cho IH, Bhandari P, Patel P, Irudayaraj J. 2015. Membrane filter–assisted surface-enhanced Raman spectroscopy for the rapid detection of *E. coli* O157: H7 in ground beef. Biosens Bioelectron 64:171–6.

Cialla D, März A, Böhme R, Theil F, Weber K, Schmitt M, Popp J. 2012. Surface-enhanced Raman spectroscopy (SERS): progress and trends. Anal Bioanal Chem 403:27–54.

Cowcher DP, Xu Y, Goodacre R. 2013. Portable, quantitative detection of bacillus bacterial spores using surface-enhanced Raman scattering. Anal Chem 85:3297–302.

Dai Q, Cheng J-H, Sun D-W, Zhu Z, Pu H. 2016. Prediction of total volatile basic nitrogen contents using wavelet features from visible/near-infrared hyperspectral images of prawn (Metapenaeus ensis). Food Chemistry 197:257–65.

Das RS, Agrawal Y. 2011. Raman spectroscopy: recent advancements, techniques and applications. Vib Spectrosc 57:163–76.

Davis R, Mauer L. 2010. Fourier transform infrared (FT-IR) spectroscopy: A rapid tool for detection and analysis of foodborne pathogenic bacteria. Curr Res Technol Educ Top Appl Microbiol Microb Biotechnol 2: 1582–94.

Davis R, Mauer LJ. 2011. Subtyping of Listeria monocytogenes at the haplotype level by Fourier transform infrared (FT-IR) spectroscopy and multivariate statistical analysis. Intl J Food Microbiol 150:140–9.

Delgado AE, Sun D-W. 2002. Desorption isotherms and glass transition temperature for chicken meat. Journal of Food Engineering 55:1–8.

Dijkstra R, Ariese F, Gooijer C, Brinkman UT. 2005. Raman spectroscopy as a detection method for liquid-separation techniques. TrAC Trend Anal Chem 24:304–23.

Dissing BS, Papadopoulou OS, Tassou C, Ersbøll BK, Carstensen JM, Panagou EZ, Nychas GJ. 2013. Using multispectral imaging for spoilage detection of pork meat. Food Bioprocess Tech 6:2268–79.

Du CJ, Sun D-W. 2005. Pizza sauce spread classification using colour vision and support vector machines. Journal of Food Engineering 66:137–45.

Duan C, Chen C, Khan MN, Liu Y, Zhang R, Lin H, Cao L. 2014. Nondestructive determination of the total bacteria in flounder fillet by portable near infrared spectrometer. Food Control 42:18–22.

Duan N, Chang B, Zhang H, Wang Z, Wu S. 2016a. *Salmonella typhimurium* detection using a surface-enhanced Raman scattering-based aptasensor. Intl J Food Microbiol 218:38–43.

Duan N, Shen M, Wu S, Zhao C, M X, Wang Z. 2017. Graphene oxide wrapped Fe3O4@ Au nanostructures as substrates for aptamer-based detection of *Vibrio parahaemolyticus* by surface-enhanced Raman spectroscopy. Microchim Acta 184:2653–60.

Duan N, Yan Y, Wu S, Wang Z. 2016b. *Vibrio parahaemolyticus* detection aptasensor using surface-enhanced Raman scattering. Food Control 63:122–7.

ElMasry G, Kamruzzaman M, Sun D-W, Allen P. 2012. Principles and applications of hyperspectral imaging in quality evaluation of agro-food products: a review. Crit Rev Food Sci 52:99–1023.

ElMasry G, Sun D-W, Allen P. 2013. Chemical-free assessment and mapping of major constituents in beef using hyperspectral imaging. Journal of Food Engineering 117:235–46.

Fan C, Hu Z, Mustapha A, Lin M. 2011. Rapid detection of food- and waterborne bacteria using surface-enhanced Raman spectroscopy coupled with silver nanosubstrates. Appl Microbiol Biot 92:1053–61.

Feng YZ, ElMasry G, Sun D-W, Scannell AG, Walsh D, Morcy N. 2013. Near-infrared hyperspectral imaging and partial least squares regression for rapid and reagentless determination of *Enterobacteriaceae* on chicken fillets. Food Chem 138:1829–36.

Feng YZ, Sun D-W. 2013a. Determination of total viable count (TVC) in chicken breast fillets by near-infrared hyperspectral imaging and spectroscopic transforms. Talanta 105:244–9.

Feng YZ, Sun D-W. 2013b. Near-infrared hyperspectral imaging in tandem with partial least squares regression and genetic algorithm for nondestructive determination and visualization of *Pseudomonas* loads in chicken fillets. Talanta 109:74–83.

Fleischmann M, Hendra PJ, McQuillan AJ. 1974. Raman spectra of pyridine adsorbed at a silver electrode. Chem Phys Lett 26:163–6.

Freiwald A, Sauer S. 2009. Phylogenetic classification and identification of bacteria by mass spectrometry. Nat Protoc 4:732–42.

Fröhling A, Klocke S, Hausdorf L, Klocke M, Schlüter O. 2012. A method for viability testing of *Pectobacterium carotovorum* in postharvest processing by means of flow cytometry. Food Bioprocess Tech 5:2871-9.

Gamble GR, Park B, Yoon SC, Lawrence KC. 2016. Effect of sample preparation on the discrimination of bacterial isolates cultured in liquid nutrient media using laser-induced breakdown spectroscopy (LIBS). Appl spectrosc 70:494–504.

Gaston E, Frias JM, Cullen PJ, O'Donnell C, Gowen A. 2011. Hyperspectral imaging for the detection of microbial spoilage of mushrooms. Paper presented at the 11th International Conference of Engineering and Food, Athens, Greece, May 22–26, 2011.

Globus T, Dorofeeva T, Sizov I, Gelmont B, Lvovska M, Khromova T, Chertihin O, Koryakina Y. 2012. Sub-THz vibrational spectroscopy of bacterial cells and molecular components. Am J Biomed Eng 2:143–54.

Gowen AA, Feng Y, Gaston E, Valdramidis V. 2015. Recent applications of hyperspectral imaging in microbiology. Talanta 137:43–54.

Harmon RS, Russo RE, Hark RR. 2013. Applications of laser-induced breakdown spectroscopy for geochemical and environmental analysis: A comprehensive review. Spectrochim Acta B 87:11–26.

He L, Deen BD, Pagel AH, Diez-Gonzalez F, Labuza TP. 2013. Concentration, detection and discrimination of *Bacillus anthracis* spores in orange juice using aptamer based surface enhanced Raman spectroscopy. Analyst 138:1657–9.

He HJ, Sun D-W, Wu D. 2014. Rapid and real-time prediction of lactic acid bacteria (LAB) in farmed salmon flesh using near-infrared (NIR) hyperspectral imaging combined with chemometric analysis. Food Res Intl 62:476–83.

Hennigan SL, Driskell JD, Ferguson-Noel N, Dluhy RA, Zhao Y, Tripp RA, Krause DC. 2012. Detection and differentiation of avian mycoplasmas by surface-enhanced Raman spectroscopy based on a silver nanorod array. Appl Environ Microb 78:1930–5.

Herrero AM. 2008. Raman spectroscopy for monitoring protein structure in muscle food systems. Crit Rev Food Sci 48:512–23.

Huang L, Zhao J, Chen Q, Zhang Y. 2013. Rapid detection of total viable count (TVC) in pork meat by hyperspectral imaging. Food Res Intl 54:821–8.

Jackman P, Sun D-W, Allen P. 2009. Automatic segmentation of beef longissimus dorsi muscle and marbling by an adaptable algorithm. Meat Science 83:187–94.

Jackman P, Sun D-W, Allen P. 2011. Recent advances in the use of computer vision technology in the quality assessment of fresh meats. Trends in Food Science & Technology 22:185–97.

Kammies TL, Manley M, Gouws PA, Williams PJ. 2016. Differentiation of foodborne bacteria using NIR hyperspectral imaging and multivariate data analysis. Appl Microbiol Biot 100:9305–20.

Kiani H, Sun D-W, Delgado A, Zhang Z. 2012. Investigation of the effect of power ultrasound on the nucleation of water during freezing of agar gel samples in tubing vials. Ultrasonics Sonochemistry 19:576–81.

Kiani H, Zhang Z, Delgado A, Sun D-W. 2011. Ultrasound assisted nucleation of some liquid and solid model foods during freezing. Food Research International 44:2915–21.

Knauer M, Ivleva NP, Niessner R, Haisch C. 2012. A flow-through microarray cell for the online SERS detection of antibody-captured *E. coli* bacteria. Anal Bioanal Chem 402:2663–7.

Kodogiannis VS. 2017. Application of an electronic nose coupled with fuzzy-wavelet network for the detection of meat spoilage. Food Bioprocess Tech 10:730–49.

Kurita I, Suzuki T, Kondo N, Kondo T, Kamba S, Miura Y, Ogawa Y. 2014. Specific detection of *Escherichia coli* by using metallic mesh sensor in THz region. In General Assembly and Scientific Symposium (URSI GASS), 2014 XXXIth URSI, (pp. 1–4): IEEE.

Lee KM, Herrman TJ. 2016. Determination and prediction of fumonisin contamination in maize by surface-enhanced Raman spectroscopy (SERS). Food Bioprocess Tech 9(4):588–603.

Li J-L, Sun D-W, Pu H, Jayas DS. 2017. Determination of trace thiophanate-methyl and its metabolite carbendazim with teratogenic risk in red bell pepper (Capsicumannuum L.) by surface-enhanced Raman imaging technique. Food Chemistry 218:543–52.

Lin M, Al-Holy M, Al-Qadiri H, Kang DH, Cavinato AG, Huang Y, Rasco BA. 2004. Discrimination of intact and injured *Listeria monocytogenes* by Fourier transform infrared spectroscopy and principal component analysis. J Agr Food Chem 52(19):5769–72.

Liu TY, Chen Y, Wang HH, Huang YL, Chao YC, Tsai KT, Cheng WC, Chuang CY, Tsai YH, Huang CY. 2012. Differentiation of bacteria cell wall using Raman scattering enhanced by nanoparticle array. J Nanosci Nanotechno 12:5004–8.

Lu X, Al-Qadiri HM, Lin M, Rasco BA. 2011. Application of mid-infrared and Raman spectroscopy to the study of bacteria. Food Bioprocess Tech 4(6):919–35.

Lu X, Samuelson DR, Xu Y, Zhang H, Wang S, Rasco BA, Xu J, Konkel ME. 2013. Detecting and tracking nosocomial methicillin-resistant *Staphylococcus aureus* using a microfluidic SERS biosensor. Anal Chem 85:2320–7.

Ma X, Liu Y, Zhou N, Duan N, Wu S, Wang Z. 2016. SERS aptasensor detection of *Salmonella typhimurium* using a magnetic gold nanoparticle and gold nanoparticle based sandwich structure. Anal Methods-UK 8: 8099–105.

Ma J, Pu H, Sun D-W, Gao W, Qu J-H, Ma K-Y. 2015. Application of Vis-NIR hyperspectral imaging in classification between fresh and frozen-thawed pork Longissimus Dorsi muscles. International Journal of Refrigeration-Revue Internationale Du Froid 50:10–8.

Ma J, Sun D-W, Q J-H, Pu H. 2017. Prediction of textural changes in grass carp fillets as affected by vacuum freeze drying using hyperspectral imaging based on integrated group wavelengths. Lwt-Food Science and Technology 82:377–85.

Ma J, Sun D-W, Pu H. 2016. Spectral absorption index in hyperspectral image analysis for predicting moisture contents in pork longissimus dorsi muscles. Food Chemistry 197:848–54.

Ma F, Yao J, Xie T, Liu C, Chen W, Chen C, Zheng L. 2014. Multispectral imaging for rapid and nondestructive determination of aerobic plate count (APC) in cooked pork sausages. Food Res Intl 62:902–8.

Madiyar FR, Bhana S, Swisher LZ, Culbertson CT, Huang X, Li J. 2015. Integration of a nanostructured dielectrophoretic device and a surface-enhanced Raman probe for highly sensitive rapid bacteria detection. Nanoscale 7:3726–36.

Magliulo M, Simoni P, Guardigli M, Michelini E, Luciani M, Lelli R, Roda A. 2007. A rapid multiplexed chemiluminescent immunoassay for the detection of *Escherichia coli* O157: H7, *Yersinia enterocolitica*, *Salmonella typhimurium*, and *Listeria monocytogenes* pathogen bacteria. J Agr Food Chem 55:4933–9.

Mantsch HH, Naumann D. 2010. Terahertz spectroscopy: The renaissance of far infrared spectroscopy. J Mol Struct 964:1–4.

Manzoor S, Moncayo S, Navarro-Villoslada F, Ayala JA, Izquierdo-Hornillos R, de Villena FM, Caceres JO. 2014. Rapid identification and discrimination of bacterial strains by laser-induced breakdown spectroscopy and neural networks. Talanta 121:65–70.

Manzoor S, Ugena L, Tornero-Lopéz J, Martín H, Molina M, Camacho JJ, Cáceres JO. 2016. Laser-induced breakdown spectroscopy for the discrimination of Candida strains. Talanta 155:101–6.

Marcos-Martinez D, Ayala JA, Izquierdo-Hornillos RC, de Villena FM, Caceres JO. 2011. Identification and discrimination of bacterial strains by laser-induced breakdown spectroscopy and neural networks. Talanta 84:730–7.

Mazhorova A, Markov A, Ng A, Chinnappan R, Skorobogata O, Zourob M, Skorobogatiy M. 2012. Label-free bacteria detection using evanescent mode of a suspended core terahertz fiber. Opt Express 20:5344–55.

McDonald K, Sun D-W, Kenny T. 2001. The effect of injection level on the quality of a rapid vacuum cooled cooked beef product. Journal of Food Engineering 47:139–47.

Miziolek AW, Palleschi V, Schechter I. (Eds.). 2006. Laser induced breakdown spectroscopy. Cambridge University Press.

Multari RA, Cremers DA, Dupre JAM, Gustafson JE. 2013. Detection of biological contaminants on foods and food surfaces using laser-induced breakdown spectroscopy (LIBS). J Agr Food Chem 61:8687–94.

Mungroo NA, Oliveira G, Neethirajan S. 2016. SERS based point-of-care detection of food-borne pathogens. Microchim Acta 183:697–707.

Najafi R, Mukherjee S, Hudson J, Sharma A, Banerjee P. 2014. Development of a rapid capture-cum-detection method for *Escherichia coli* O157 from apple juice comprising nano-immunomagnetic separation in tandem with surface enhanced Raman scattering. Intl J Food Microbiol 189:89–97.

Ok G, Kim HJ, Chun HS, Choi SW. 2014. Foreign-body detection in dry food using continuous sub-terahertz wave imaging. Food Control 42: 284–9.

Olaoye OA, Onilude AA, Idowu OA. 2011. Microbiological profile of goat meat inoculated with lactic acid bacteria cultures and stored at 30 C for 7 days. Food Bioprocess Tech 4:312—9.

Ozaki Y, McClure WF, Christy AA. 2006. Near-infrared spectroscopy in food science and technology. John Wiley & Sons.

Panagou EZ, Papadopoulou O, Carstensen JM, Nychas GJE. 2014. Potential of multispectral imaging technology for rapid and nondestructive determination of the microbiological quality of beef filets during aerobic storage. Intl J Food Microbiol 174:1–11.

Papadopoulou O, Panagou E, Tassou C, Nychas GJ. 2011. Contribution of Fourier transform infrared (FTIR) spectroscopy data on the quantitative determination of minced pork meat spoilage. Food Res Intl 44:3264–71.

Park S, Hong J, Choi S, Kim H, Park W, Han S, Park J, Lee S, Kim D, Ahn Y. 2014a. Detection of microorganisms using terahertz metamaterials. Sci Rep-UK 4:4988.

Park MK., Li S, Chin BA. 2013. Detection of *Salmonella typhimurium* grown directly on tomato surface using phage-based magnetoelastic biosensors. Food Bioprocess Tech 6:682–9.

Park B, Seo YW, Yoon SC, Jr AH, Windham WR, Lawrence KC. 2015. Hyperspectral microscope imaging methods to classify Gram-positive and Gram-negative foodborne pathogenic bacteria. Trans ASABE 58(1):5–16.

Park S, Son B, Choi S, Kim H, Ahn Y. 2014b. Sensitive detection of yeast using terahertz slot antennas. Opt Express 22:30467–72.

Peng Y, Zhang J, Wang W, Li Y, Wu J, Huang H, Gao X, Jiang W. 2011. Potential prediction of the microbial spoilage of beef using spatially resolved hyperspectral scattering profiles. J Food Eng, 102:163–9.

Pu H, Kamruzzaman M, Sun D-W. 2015. Selection of feature wavelengths for developing multispectral imaging systems for quality, safety and authenticity of muscle foods-a review. Trends Food Sci Tech 45:86–104.

Pu H, Kamruzzaman M, Sun D-W. 2015. Selection of feature wavelengths for developing multispectral imaging systems for quality, safety and authenticity of muscle foods-a review. Trends in Food Science & Technology 45:86–104.

Pu H, Liu D, Wang L, Sun D-W. 2016. Soluble solids content and pH prediction and maturity discrimination of lychee fruits using visible and near infrared hyperspectral imaging. Food Analytical Methods 9:235–44.

Pu Y-Y, Sun D-W. 2016. Prediction of moisture content uniformity of microwave-vacuum dried mangoes as affected by different shapes using NIR hyperspectral imaging. Innovative Food Science & Emerging Technologies 33:348–56.

Pu Y-Y, Sun D-W. 2017. Combined hot-air and microwave-vacuum drying for improving drying uniformity of mango slices based on hyperspectral imaging visualisation of moisture content distribution. Biosystems Engineering 156:108–19.

Pu H, Sun D-W, Ma J, Cheng J-H. 2015. Classification of fresh and frozen-thawed pork muscles using visible and near infrared hyperspectral imaging and textural analysis. Meat Science 99:81–8.

Pu H, Xie A, Sun D-W, Kamruzzaman M, Ma J. 2015. Application of wavelet analysis to spectral data for categorization of lamb muscles. Food and Bioprocess Technology 8:1–16.

Putnam RA, Mohaidat QI, Daabous A, Rehse SJ. 2013. A comparison of multivariate analysis techniques and variable selection strategies in a laser-induced breakdown spectroscopy bacterial classification. Spectrochim Acta B 87:161–7.

Qu J-H, Sun D-W, Cheng J-H, Pu H. 2017. Mapping moisture contents in grass carp (Ctenopharyngodon idella) slices under different freeze drying periods by Vis-NIR hyperspectral imaging. Lwt-Food Science and Technology 75:529–36.

Ravikanth L, Jayas DS, White ND, Fields PG, Sun D-W. 2017. Extraction of spectral information from hyperspectral data and application of hyperspectral imaging for food and agricultural products. Food Bioprocess Tech 10(1):1–33.

Shapaval V, Møretrø T, Wold Åsli A, Suso HP, Schmitt J, Lillehaug D, Kohler A. 2016. A novel library-independent approach based on high-throughput cultivation in bioscreen and fingerprinting by FTIR spectroscopy for microbial source tracking in food industry. Lett Appl Microbiol 64:335–42.

Shapaval V, Schmitt J, Møretrø T, Suso HP, Skaar I, AW Å, Lillehaug D, Kohler A. 2013a. Characterization of food spoilage fungi by FTIR spectroscopy. J Appl Microbiol 114:788–96.

Shapaval V, Walczak B, Gognies S, Suso HP, Belarbi A, Kohler A. 2013b. FTIR spectroscopic characterization of differently cultivated food-related yeasts. Analyst 138:4129–38.

Sharma B, Frontiera RR, Henry AI, Ringe E, Van Duyne RP. 2012. SERS: materials, applications, and the future. Mater Today 15:16–25.

Siripatrawan U, Makino Y, Kawagoe Y, Oshita S. 2011. Rapid detection of *Escherichia coli* contamination in packaged fresh spinach using hyperspectral imaging. Talanta 85:276–81.

Sivakumar P, Fernández-Bravo A, Taleh L, Biddle JF, Melikechi N. 2015. Detection and classification of live and dead *Escherichia coli* by laser-induced breakdown spectroscopy. Astrobiology 15:144–53.

Spizzichino V, Fantoni R. 2014. Laser-induced breakdown spectroscopy in archeometry: A review of its application and future perspectives. Spectrochim Acta B 99:201–9.

Stevens KA, Jaykus LA. 2004. Bacterial separation and concentration from complex sample matrices: a review. Crit Rev Microbiol 30:7–24.

Sundaram J, Park B, Kwon Y, Lawrence KC. 2013. Surface enhanced Raman scattering (SERS) with biopolymer encapsulated silver nanosubstrates for rapid detection of foodborne pathogens. Intl J Food Microbiol 167:67–73.

Sun D-W. 1997. Solar powered combined ejector vapour compression cycle for air conditioning and refrigeration. Energy Conversion and Management 38:479–91.

Sun D-W. 1999. Comparison and selection of EMC ERH isotherm equations for rice. Journal of Stored Products Research 35:249–64.

Sun D-W. 2004. Computer vision - An objective, rapid and non-contact quality evaluation tool for the food industry. Journal of Food Engineering 61:1–2.

Sun D-W, Brosnan T. 2003. Pizza quality evaluation using computer vision - Part 2 - Pizza topping analysis. Journal of Food Engineering 57:91–5.

Sun D-W, Zheng LY. 2006. Vacuum cooling technology for the agri-food industry: Past, present and future. Journal of Food Engineering 77:203–14.

Tao F, Peng Y. 2015. A nondestructive method for prediction of total viable count in pork meat by hyperspectral scattering imaging. Food Bioprocess Tech 8:17–30.

Tao F, Peng Y, Li Y, Chao K, Dhakal S. 2012. Simultaneous determination of tenderness and *Escherichia coli* contamination of pork using hyperspectral scattering technique. Meat Sci 90:851–7.

Tenggara AP, Park S, Yudistira HT, Ahn Y, Byun D. 2017. Fabrication of terahertz metamaterials using electrohydrodynamic jet printing for sensitive detection of yeast. J Micromech Microeng 27:035009.

Tito N, Rodemann T, Powell S. 2012. Use of near-infrared spectroscopy to predict microbial numbers on Atlantic salmon. Food Microbiol 32:431–6.

Türker-Kaya S, Huck CW. 2017. A review of mid-infrared and near-infrared imaging: principles, concepts and applications in plant tissue analysis. Molecules 22:168.

Vikesland PJ, Wigginton KR. 2010. Nanomaterial enabled biosensors for pathogen monitoring–a review. EnvironSci Technol 44:3656–69.

Walter A, März A, Schumacher W, Rösch P, Popp J. 2011. Towards a fast, high specific and reliable discrimination of bacteria on strain level by means of SERS in a microfluidic device. Lab Chip 11:1013–21.

Wang P, Pang S, Chen J, McLandsborough L, Nugen SR, Fan M, He L. 2016c. Label-free mapping of single bacterial cells using surface-enhanced Raman spectroscopy. Analyst 141:1356–62.

Wang P, Pang S, Pearson B, Chujo Y, McLandsborough L, Fan M, He L. 2017c. Rapid concentration detection and differentiation of bacteria in skimmed milk using surface-enhanced Raman scattering mapping on 4-mercaptophenylboronic acid functionalized silver dendrites. Anal Bioanal Chem 409:2229–38.

Wang LJ, Sun D-W. 2001. Rapid cooling of porous and moisture foods by using vacuum cooling technology. Trends in Food Science & Technology 12:174–84.

Wang LJ, Sun D-W. 2004. Effect of operating conditions of a vacuum cooler on cooling performance for large cooked meat joints. Journal of Food Engineering 61:231–40.

Wang K, Sun D-W, Pu H. 2017a. Emerging non-destructive terahertz spectroscopic imaging technique: Principle and applications in the agri-food industry. Trends Food Sci Tech 67:93-105.

Wang K, Sun D-W, Pu H, Wei Q. 2017b. Principles and applications of spectroscopic techniques for evaluating food protein conformational changes: A review. Trends Food Sci Tech 67:207–19.

Wang C, Wang J, Li M, Qu X, Zhang K, Rong Z, Xiao R, Wang S. 2016a. A rapid SERS method for label-free bacteria detection using polyethylenimine-modified Au-coated magnetic microspheres and Au@Ag nanoparticles. Analyst 141:6226–38.

Wang J, Wu X, Wang C, Rong Z, Ding H, Li H, Li S, Shao N, Dong P, Xiao R, Wang S. 2016b. Facile synthesis of Au-coated magnetic nanoparticles and their application in bacteria detection via a SERS method. ACS Appl Mater Inter 8:19958–67.

Wang J, Wu X, Wang C, Shao N, Dong P, Xiao R, Wang S. 2015. Magnetically assisted surface-enhanced Raman spectroscopy for the detection of *Staphylococcus aureus* based on aptamer recognition. ACS Appl Mater Inter 7:20919–29.

Williams PJ, Geladi P, Britz TJ, Manley M. 2012. Near-infrared (NIR) hyperspectral imaging and multivariate image analysis to study growth characteristics and differences between species and strains of members of the genus *Fusarium*. Anal Bioanal Chem 404:1759–69.

Wu X, Huang YW, Park B, Tripp RA, Zhao Y. 2015. Differentiation and classification of bacteria using vancomycin functionalized silver nanorods array based surface-enhanced Raman spectroscopy and chemometric analysis. Talanta 139:96–103.

Wu D, Sun D-W. 2013. Advanced applications of hyperspectral imaging technology for food quality and safety analysis and assessment: A review—part I: Fundamentals. Innov Food Sci Emerg 19:1–14.

Wu X, Xu C, Tripp RA, Huang Yw, Zhao Y. 2013. Detection and differentiation of foodborne pathogenic bacteria in mung bean sprouts using field deployable label-free SERS devices. Analyst 138:3005–12.

Xie A, Sun D-W, Xu Z, Zhu Z. 2015. Rapid detection of frozen pork quality without thawing by Vis-NIR hyperspectral imaging technique. Talanta 139:208–15.

Xie A, Sun D-W, Zhu Z, Pu H. 2016. Nondestructive Measurements of Freezing Parameters of Frozen Porcine Meat by NIR Hyperspectral Imaging. Food and Bioprocess Technology 9:1444–54.

Xie Y, Xu L, Wang Y, Shao J, Wang L, Wang H, Qian H, Yao W. 2012. Label-free detection of the foodborne pathogens of *Enterobacteriaceae* by surface-enhanced Raman spectroscopy. Anal Methods-UK 5:946–52.

Xiong Z, Sun D-W, Pu H, Xie A, Han Z, Luo M. 2015. Non-destructive prediction of thiobarbituric acid reactive substances (TSARS) value for freshness evaluation of chicken meat using hyperspectral imaging. Food Chemistry 179:175–81.

Xu J-L, Riccioli C, Sun D-W. 2016. Development of an alternative technique for rapid and accurate determination of fish caloric density based on hyperspectral imaging. Journal of Food Engineering 190:185–94.

Xu J-L, Riccioli C, Sun D-W. 2017. Comparison of hyperspectral imaging and computer vision for automatic differentiation of organically and conventionally farmed salmon. Journal of Food Engineering 196:170–82.

Xu J-L, Sun D-W. 2017. Identification of freezer burn on frozen salmon surface using hyperspectral imaging and computer vision combined with machine learning algorithm. International Journal of Refrigeration-Revue Internationale Du Froid 74:151–64.

Xu J, Turner JW, Idso M, Biryukov SV, Rognstad L, Gong H, Trainer VL, Wells ML, Strom MS, Yu Q. 2013. In situ strain-level detection and identification of *Vibrio parahaemolyticus* using surface-enhanced Raman spectroscopy. Anal Chem 85:2630–7.

Yang Q, Sun D-W, Cheng W. 2017. Development of simplified models for nondestructive hyperspectral imaging monitoring of TVB-N contents in cured meat during drying process. Journal of Food Engineering 192:53–60.

Yang X, Wei D, Yan S, Liu Y, Yu S, Zhang M, Yang Z, Zhu X, Huang Q, Cui HL. 2016a. Rapid and label-free detection and assessment of bacteria by terahertz time-domain spectroscopy. J Biophotonics 9:1050–8.

Yang X, Zhao X, Yang K, Liu Y, Liu Y, Fu W, Luo Y. 2016b. Biomedical applications of terahertz spectroscopy and imaging. Trends Biotechnol 34:810–24.

Yoon SC, Windham WR, Ladely S, Heitschmidt GW, Lawrence KC, Park B, Narang N, Cray WC. 2013. Differentiation of big-six non-O157 Shiga-toxin producing *Escherichia coli* (STEC) on spread plates of mixed cultures using hyperspectral imaging. J Food Meas Charact 7:47–59.

Zhang WB. 2012. Review on analysis of biodiesel with infrared spectroscopy. Renew Sust Energ Rev 16:6048–58.

Zhang JY, Do J, Premasiri WR, Ziegler LD, Klapperich CM. 2010. Rapid point-of-care concentration of bacteria in a disposable microfluidic device using meniscus dragging effect. Lab Chip 10:3265–70.

Zhang H, Ma X, Liu Y, Duan N, Wu S, Wang Z, Xu B. 2015. Gold nanoparticles enhanced SERS aptasensor for the simultaneous detection of *Salmonella typhimurium* and *Staphylococcus aureus*. Biosens Bioelectron 74:872–7.

Zhang Q, Wang XD, Tian T, Chu LQ. 2017. Incorporation of multilayered silver nanoparticles into polymer brushes as 3-dimensional SERS substrates and their application for bacteria detection. Appl Surf Sci 407:185–91.

Zhou H, Yang D, Ivleva NP, Mircescu NE, Niessner R, Haisch C. 2014. SERS detection of bacteria in water by in situ coating with Ag nanoparticles. Anal Chem 86:1525–33.